Near-Infrared Spectropolarimetry at VTT and GREGOR: 25+ years of successful German-Spanish collaboration

M. Collados

Instituto de Astrofísica de Canarias
Departamento de Astrofísica, University of La Laguna

Thanks to the IAC, KIS, MPS, and AIP technical teams

Thanks to all observers

A bit of history

- **<u>1992</u>**: Request to the IAC to build an infrared polarimeter for GREGORY/VTT
  (and a visible polarimeter for SST)
- **<u>1995-1998</u>:** Development and construction of the Tenerife Infrared Polarimeter - TIP (and LPSP).
  NIR Detector: NICMOS 256 x 256 HgCdT sensor. IAC-KIS Collaboration
- **<u>1998</u>:** Commissioning of TIP at GREGORY and VTT
- **<u>1999</u>**: TIP permanently installed at VTT as a <u>common instrument</u> for all users installed
  at the Echelle spectrograph. Calibrated data offered to observers within the day.
- **<u>2005</u>:** TIP upgraded with a larger 1k detector – IAC-MPS Collaboration
- **<u>2014</u>:** TIP permanently moved to GREGOR and installed at GRIS (GREGOR Infrared
  Spectrograph). IAC-KIS-MPS-AIP Collaboration. <u>Offered as a common-use instrument.</u>
  Calibrated data offered to observers within the day and openly accessible
  through the KIS SDC (Science Data Centre) following the standard guidelines
  developed within the EU projects FP7 and H2020 SOLARNET.

The 1999-2004 TIP-I @ VTT configuration

- Polarization analyzer: 2 FLCs + BS
- NICMOS-3 256 x 256 sensor
- Spectral regions: 1.0-1.3 μm, 1.5-1.8 μm, 2-0-2.3 μm
- Spatial and Spectral sampling: 0.35” x 30 mÅ
- Spatial and Spectral intervals: 35” x 7.5 Å
- Synchronised with GFPI/TESOS/POLIS

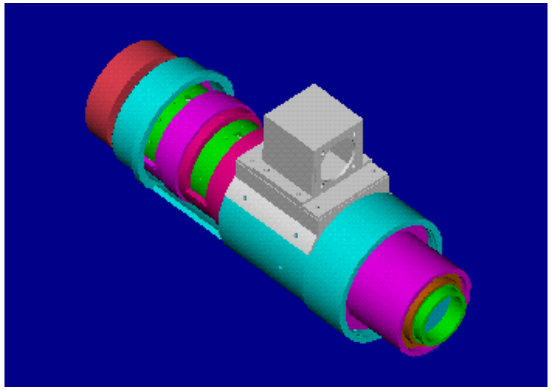

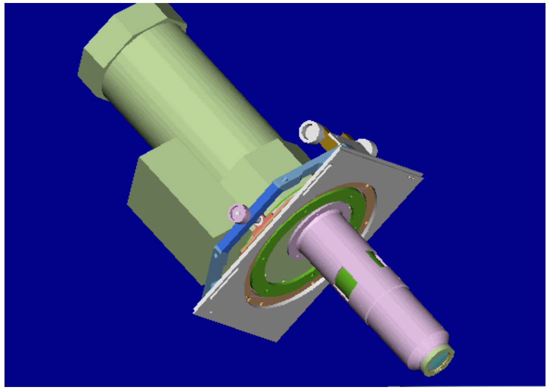

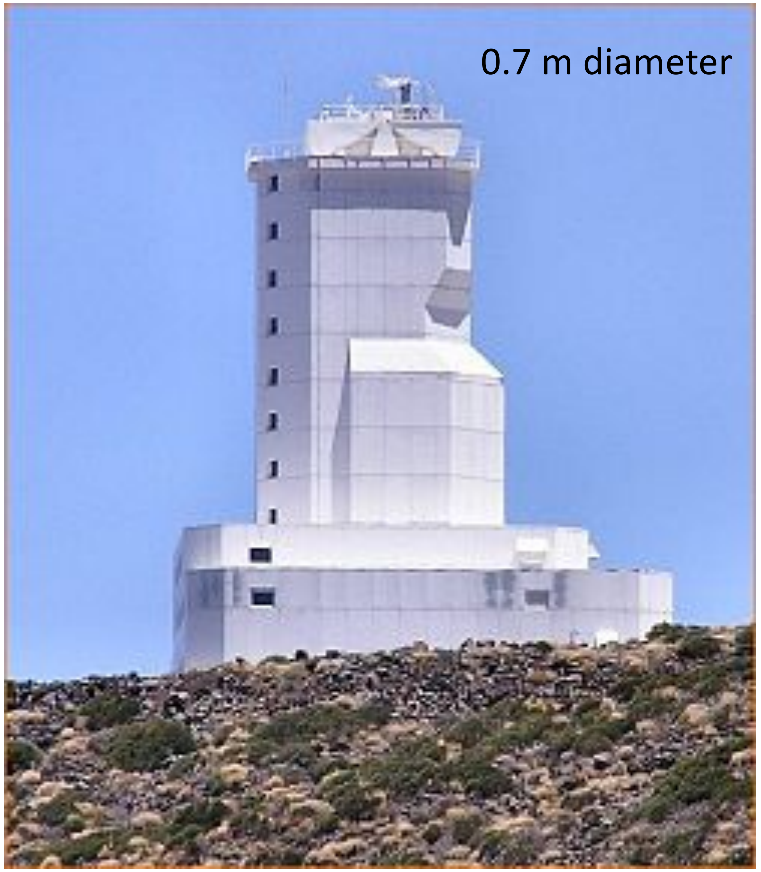

Polarimetric techniques

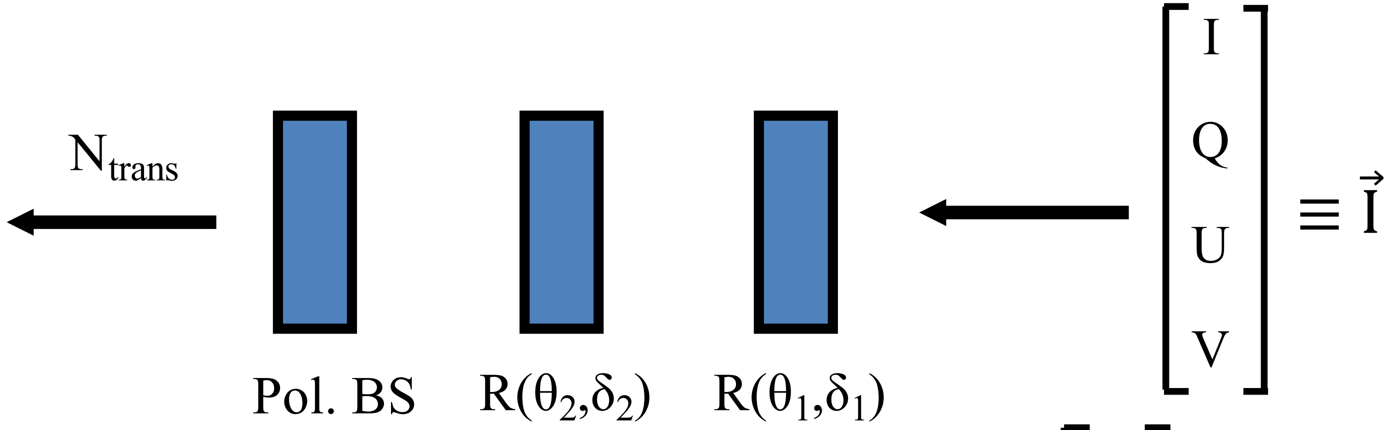

$$N_{trans} = \begin{bmatrix}1 & \pm 1 & 0 & 0\end{bmatrix} R\,(\theta_2\,,\,\delta_2)\; R\,(\theta_1\,,\,\delta_1) \begin{bmatrix} I \\ Q \\ U \\ V \end{bmatrix} \longrightarrow$$

$$\longrightarrow\; \vec{N} = \boldsymbol{M}\,\vec{I} \longrightarrow \vec{I} = \boldsymbol{D}\,\vec{N} \quad //\; \boldsymbol{D}\,\boldsymbol{M} = \boldsymbol{1}$$

Polarimetric techniques

Modulation efficiency

$$\vec{\mathrm{N}} = \boldsymbol{M}\,\vec{\mathrm{I}} \longrightarrow \vec{\mathrm{I}} = \boldsymbol{D}\,\vec{\mathrm{N}} \quad // \quad \boldsymbol{D}\,\boldsymbol{M} = \boldsymbol{1}$$

$$\epsilon_i = \left(n \sum_{j=1}^{n} {D_{ij}}^2 \right)^{-1/2} \qquad \epsilon_1 \leq 1, \qquad \sum_{i=2}^{4} {\epsilon_i}^2 \leq 1$$

del Toro Iniesta & Collados (2000)

$$\sigma_i = \frac{\sigma}{\epsilon_i}$$ Larger efficiencies mean lower noise

Optimum efficiencies

Equal efficiency for Q,U, and V

} $\epsilon_{Q,U,V} = 1/\sqrt{3} = 0.577$

The 1999-2004 TIP-I @ VTT configuration

TIP modulators: 2 ferroelectric liquid crystals

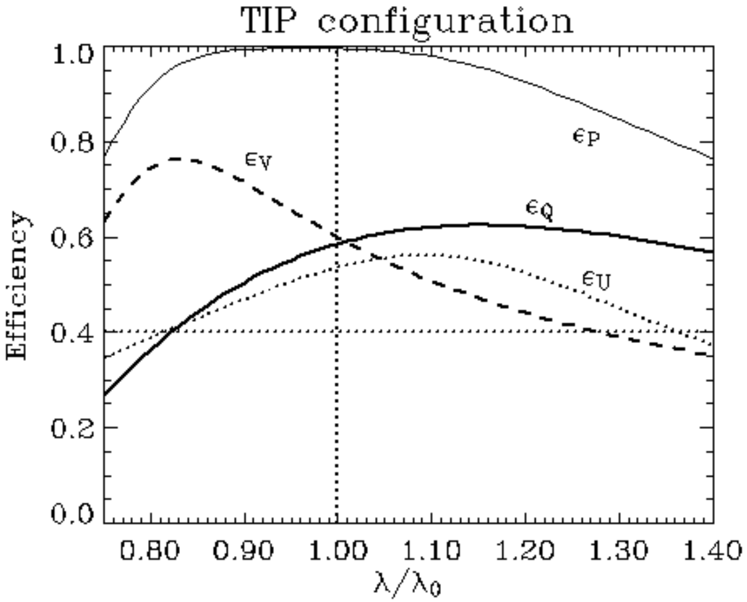

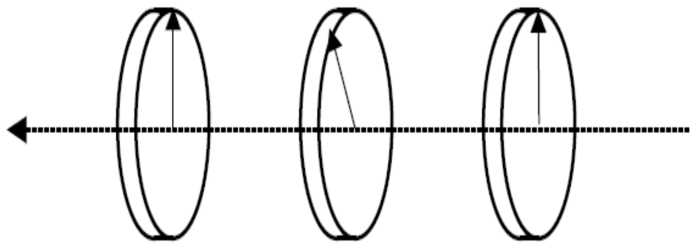

δ_1 = 155º δ_2 = 75º

θ_1 = 70º θ_2 = 155º $\Delta\theta$ = 50º

Fixed retardances

Acquired in 1995 and still working!

The 2005-2013 TIP-II @ VTT configuration

- Polarization analyzer: 2 FLCs + BS
- TCM-8600 1k x 1k sensor (MPS Collaboration)
- Spectral regions: 1.0-1.3 μm and 1.5-1.8 μm
- Spatial and Spectral sampling: 0.17” x 16 mÅ
- Spatial and Spectral intervals: 80” x 16 Å
- Synchronised with GFPI/TESOS/POLIS

- ✓ Better spatial sampling (0.17”/px vs 0.35”/px)
- ✓ Larger spatial coverage (80” vs 35”)
- ✓ Larger spectral coverage (16 Å vs 7.5 Å)

The 2005-2013 TIP-II @ VTT configuration

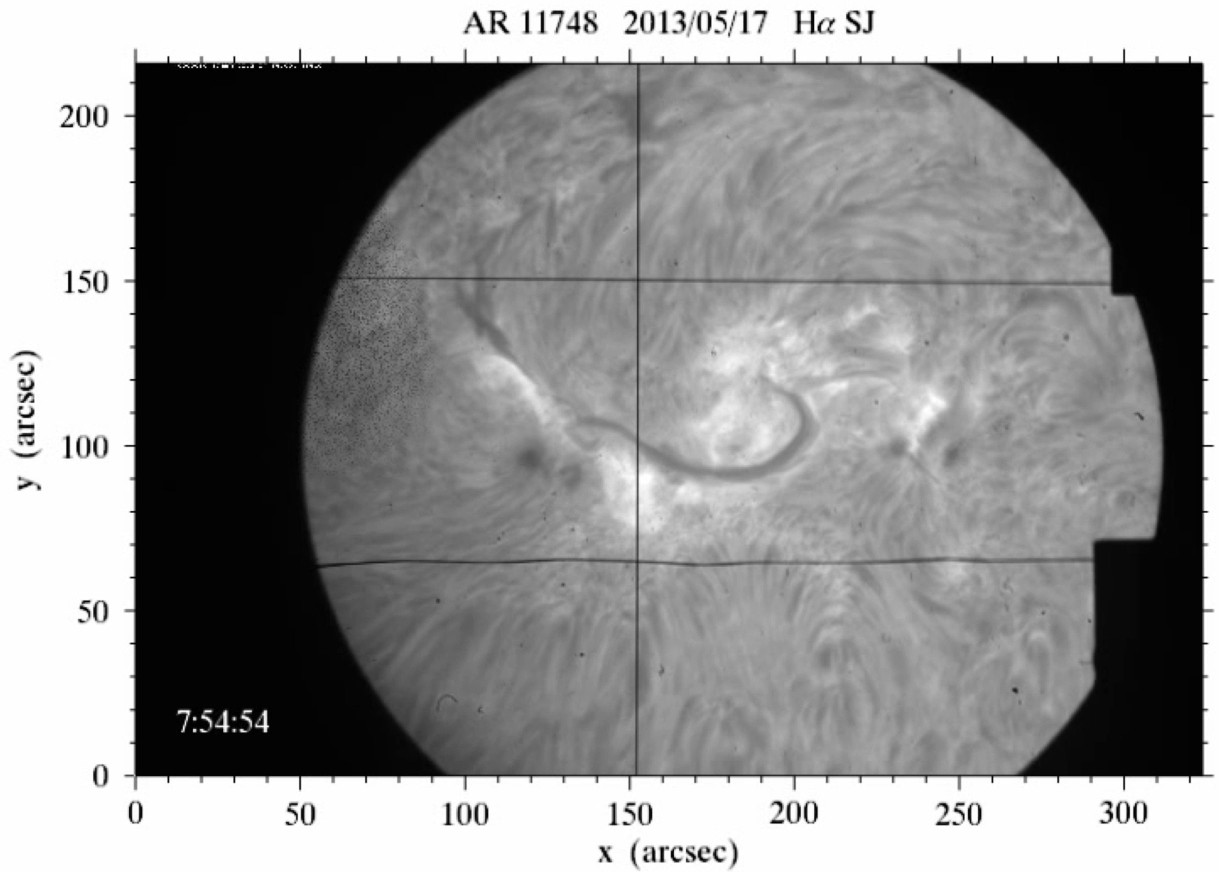

17 May 2013 // AR 11748

N11 E34 // 07:55 – 10:30 UT

Hα Slitjaw context image

M2-Flare Evolution

Kuckein et al. (2015, 2025)

The 2005-2013 TIP-II @ VTT configuration

Spectral profiles in flaring region

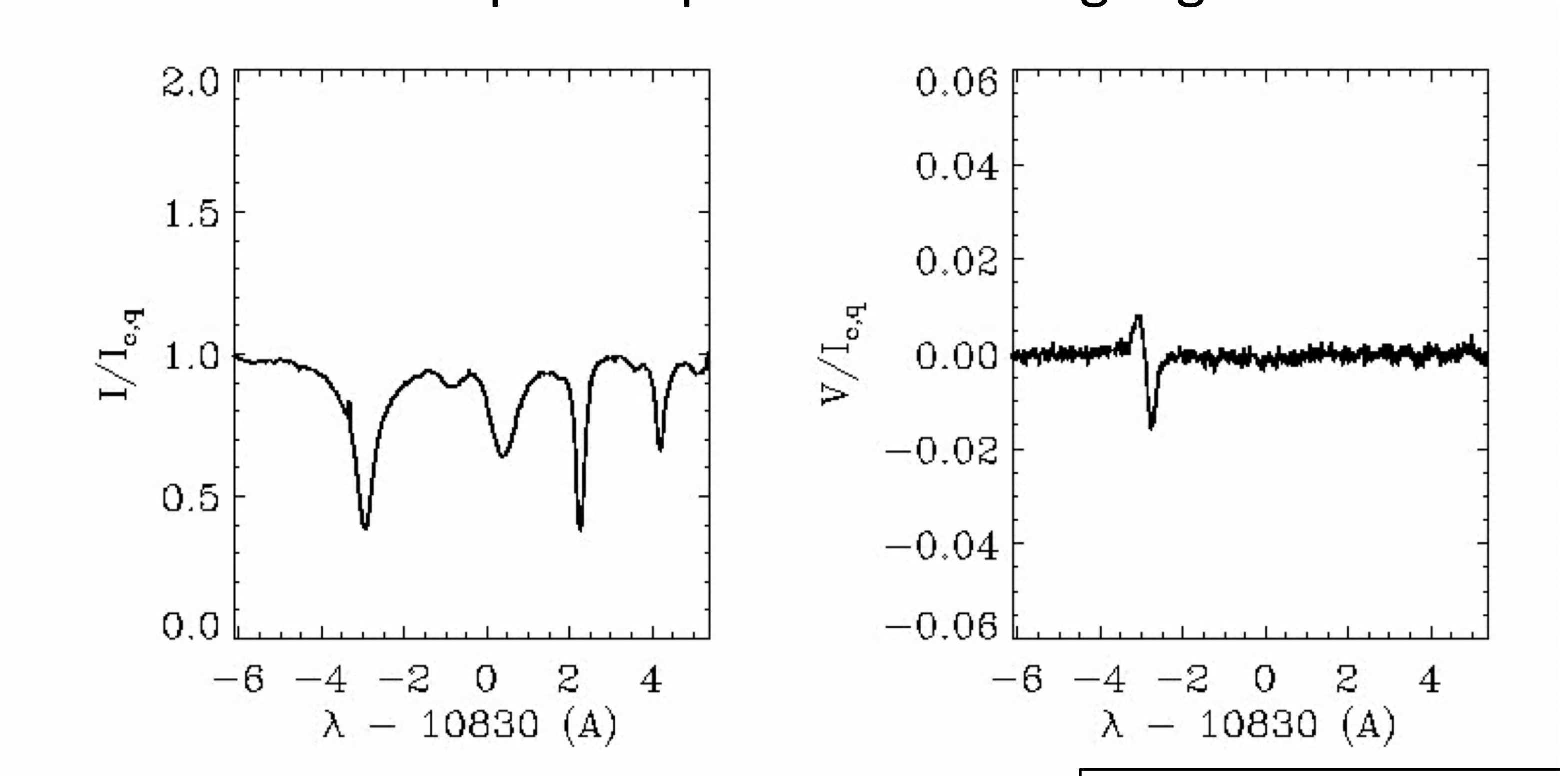

Kuckein et al. (2015, 2025)

The 2014 GREGOR Infrared Spectropolarimeter

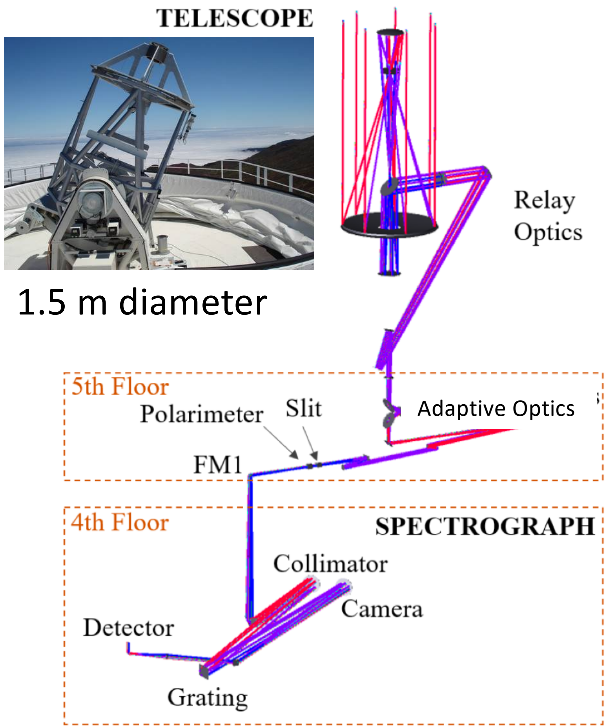

Optical path of the GREGOR telescope and the GRIS spectrograph

- Czerny-Turner based Spectrograph
- Resolving power around 1-2 x 10^5
- Scanning long-slit mode since 2014
- Spatial resolution: 0.27" (Gregor diffraction limit at 1.56 μm)

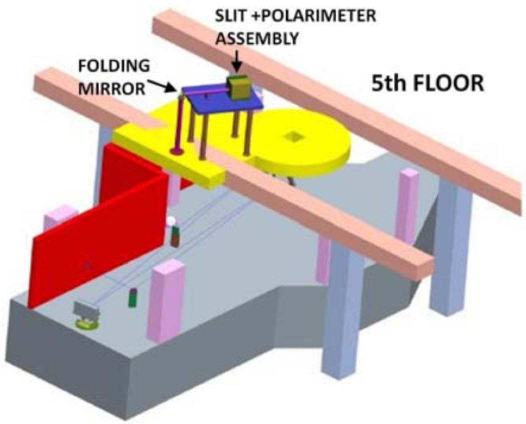

- Baseline spectral bandpass from 1 to 2.3 μm
  - 1k x 1k Rockwell sensor
- Dual-beam polarimetry (1 – 1.8 μm)
- Used in combination with GFPI/HiFI

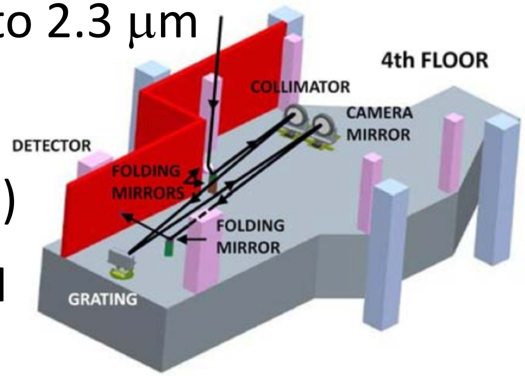

Collados et al. (2012)

Scanning slit spectrograph (2014)

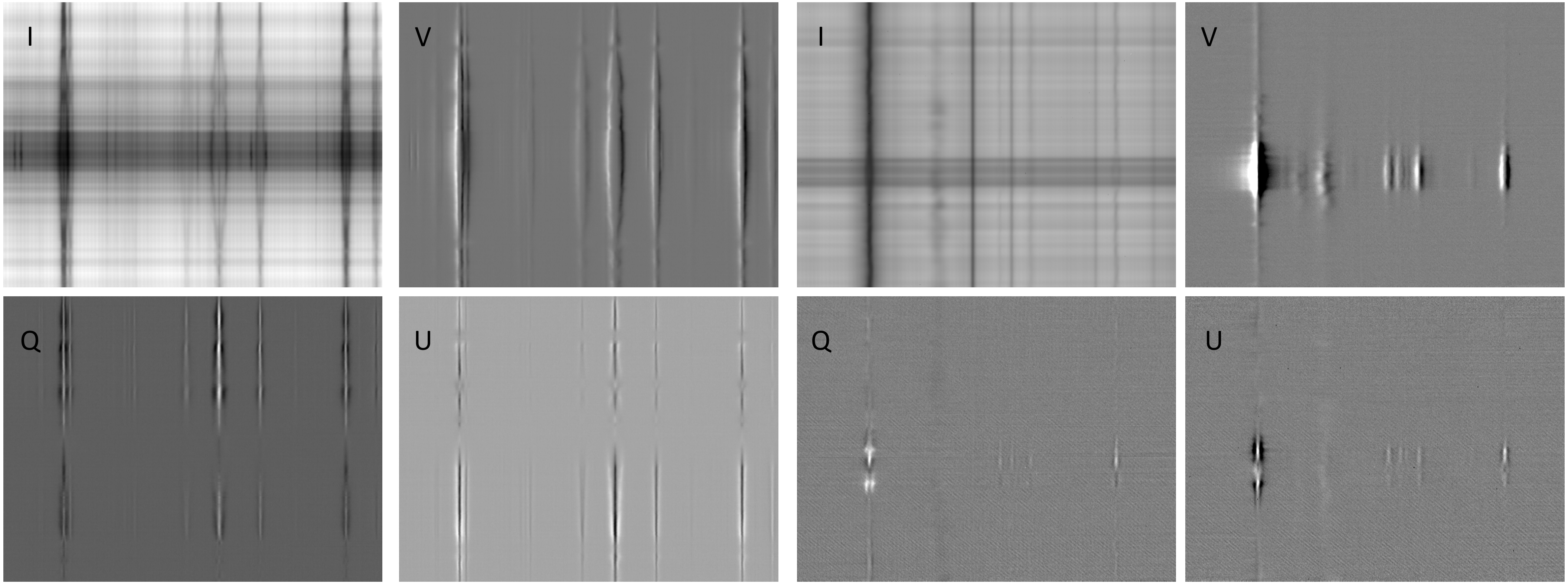

1.565 μm wavelength region

1.083 μm wavelength region

Scanning slit spectrograph (2014)

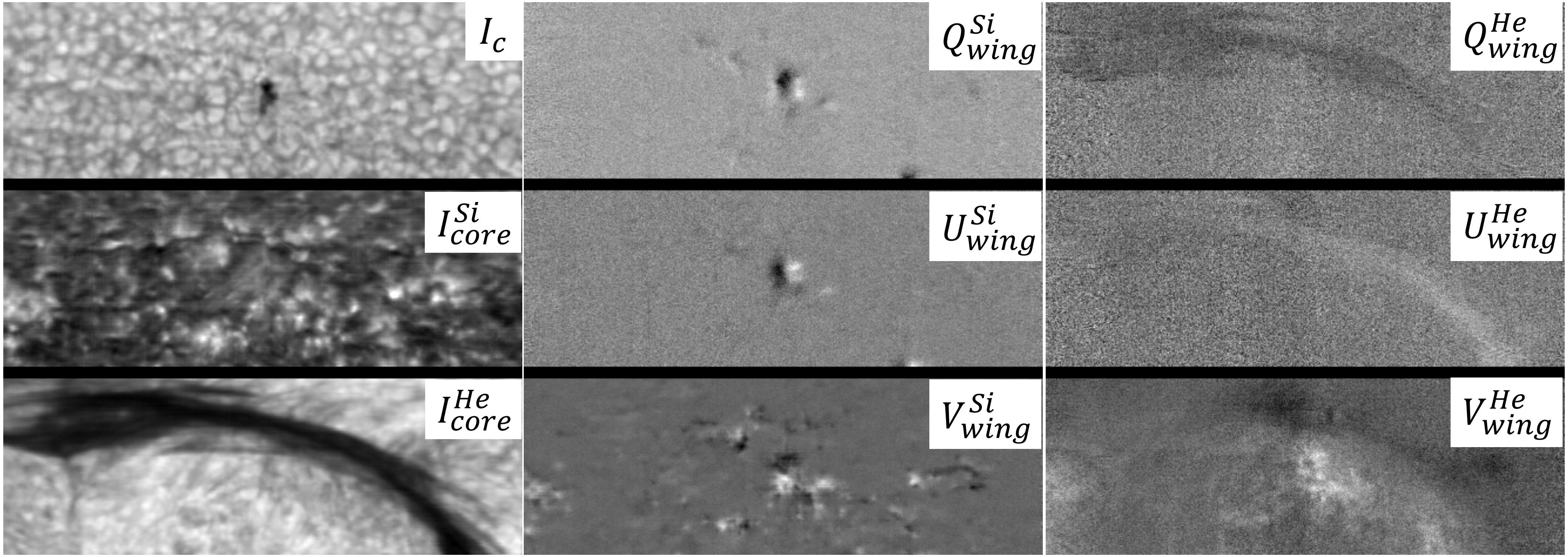

Courtesy: Ch. Kuckein

... A bit of history

- **<u>2018</u>:** Integral Field Unit installed at GRIS and offered as a common-use option.
  2D spectropolarimetry

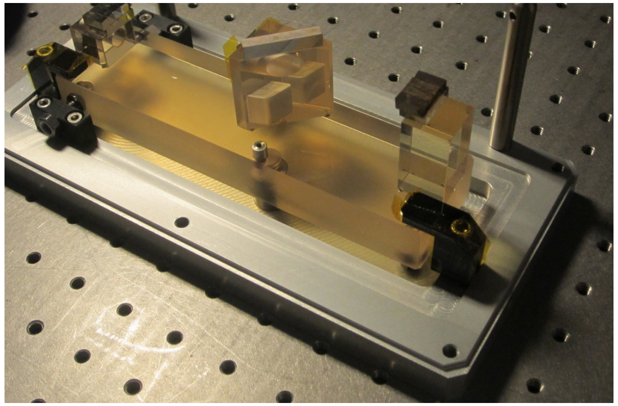

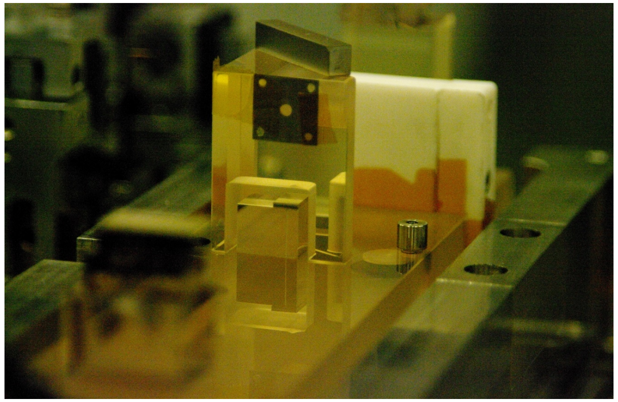

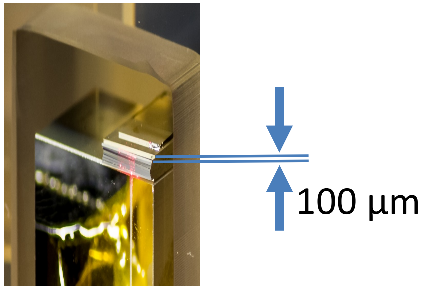

Domínguez-Tagle et al. (2018)

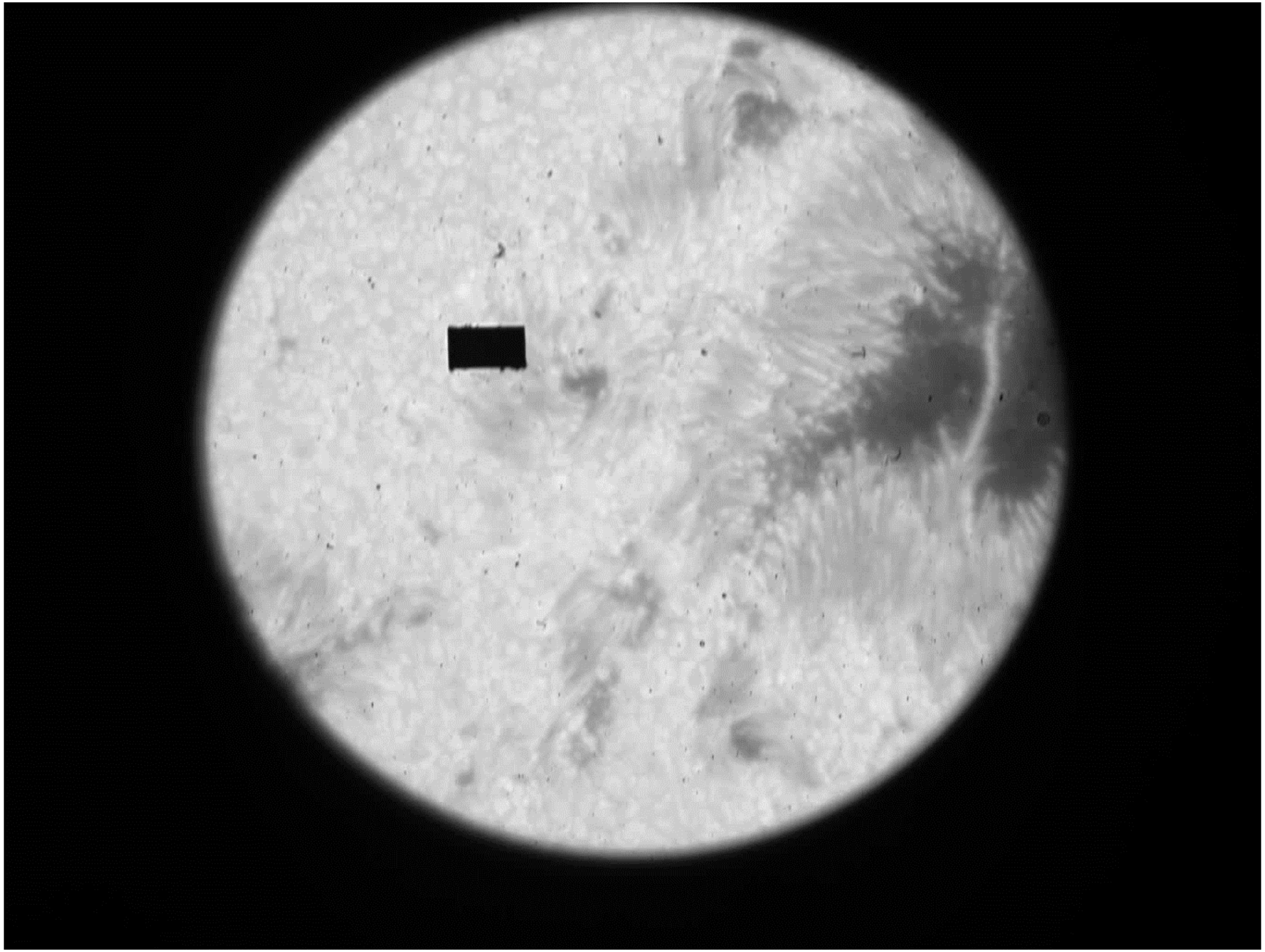

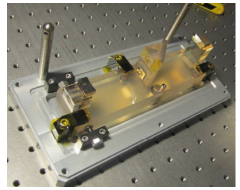

Monochromatic images

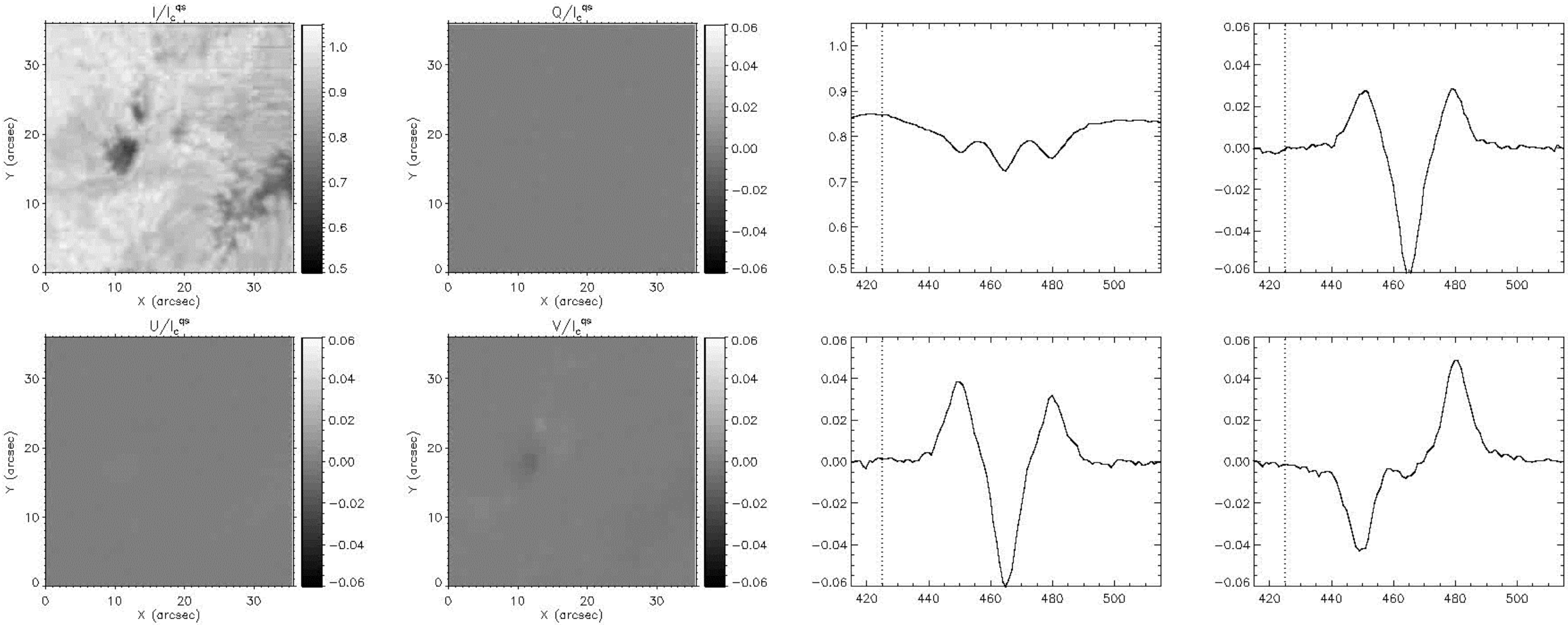

Domínguez-Tagle et al. (2022)

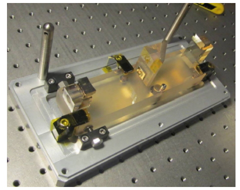

Temporal evolution

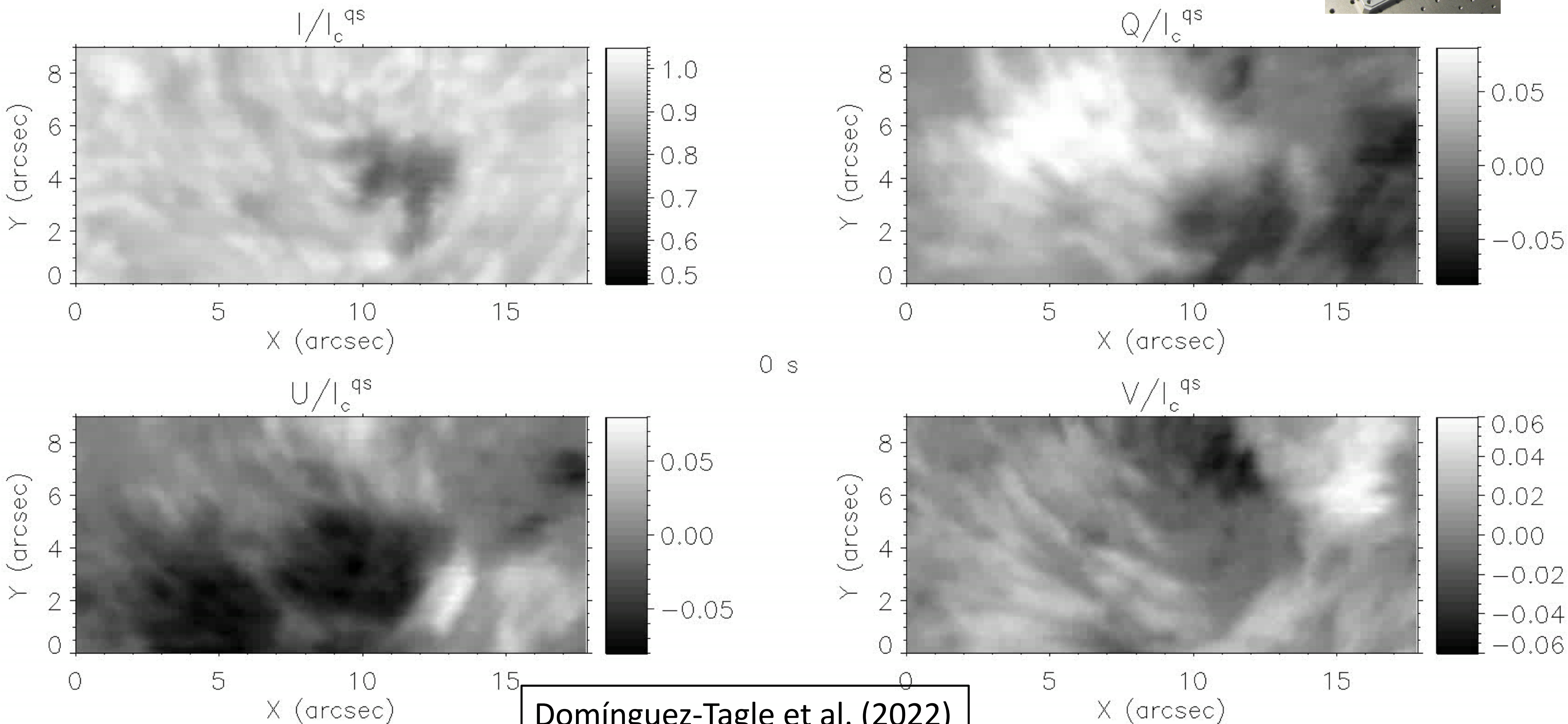

Domínguez-Tagle et al. (2022)

Fixed position integral field spectrograph

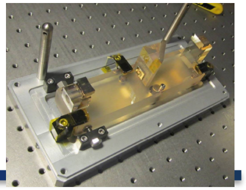

I_c maps $\quad \Delta t = 4\,s \; - t_{seq} = 2\,min \quad$ V_{wing} maps

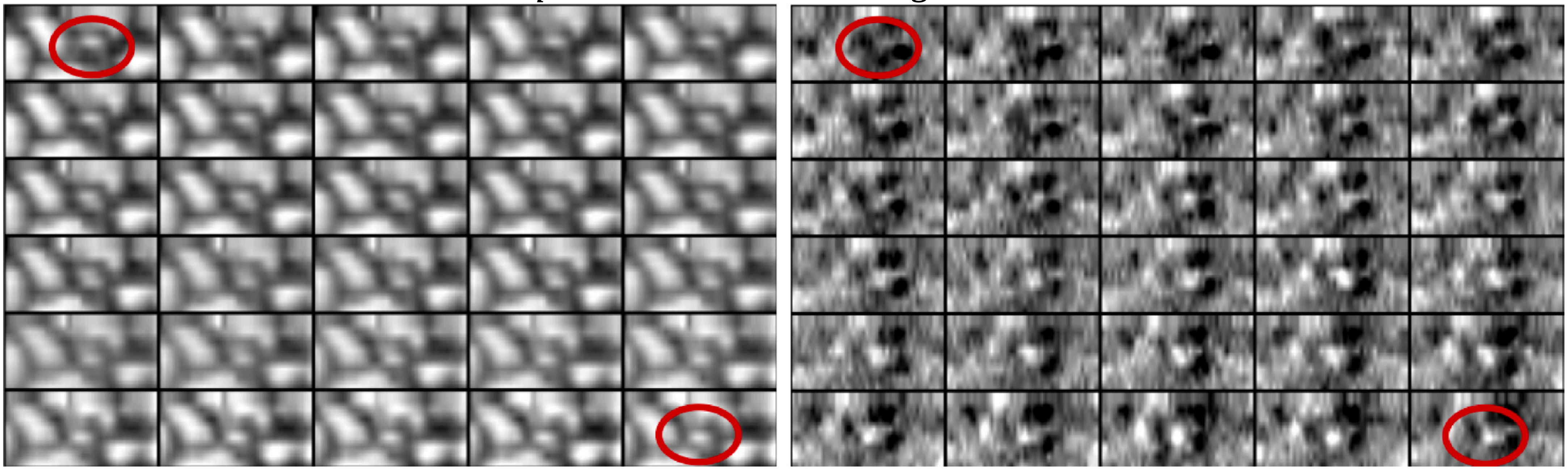

Domínguez-Tagle et al. (2022)

Upgrades@GREGOR: New transfer optics and AO optical layout (2019)

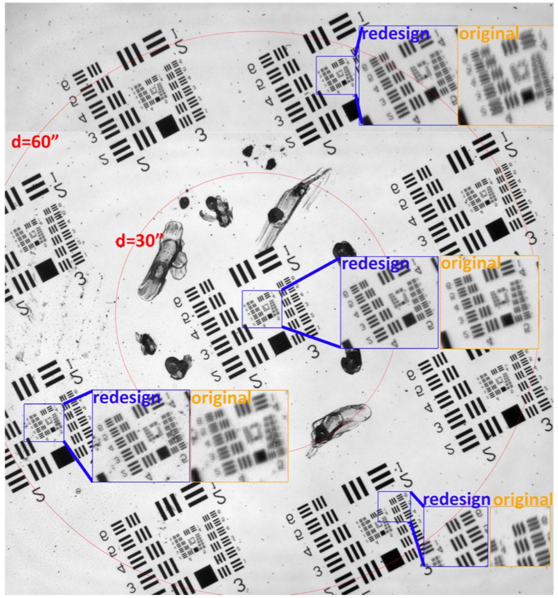

Kleint et al. (2020)

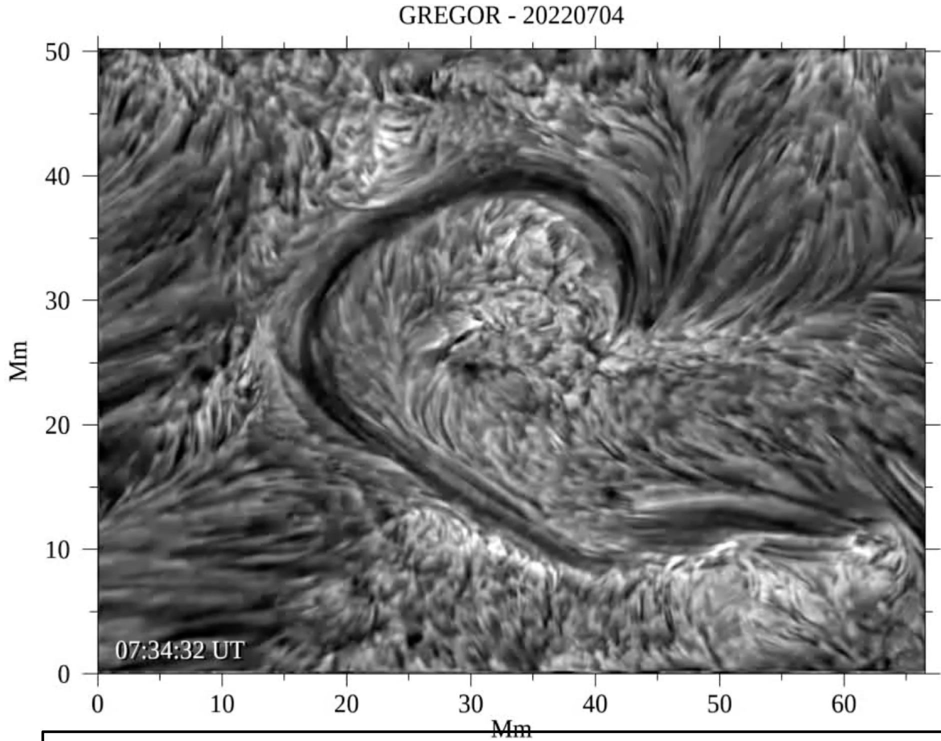

HIFI@GREGOR
courtesy of S.J. González Manrique and Ch. Kuckein

... A bit of history

<u>2024</u>: Additional simultaneous spectroscopic channels for multi-wavelength spectropolarimetry

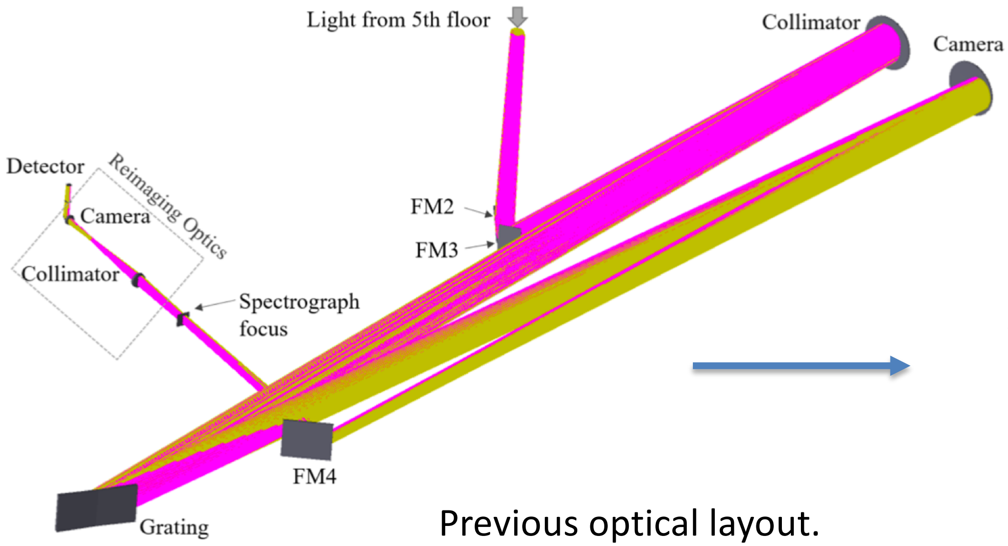

Previous optical layout.

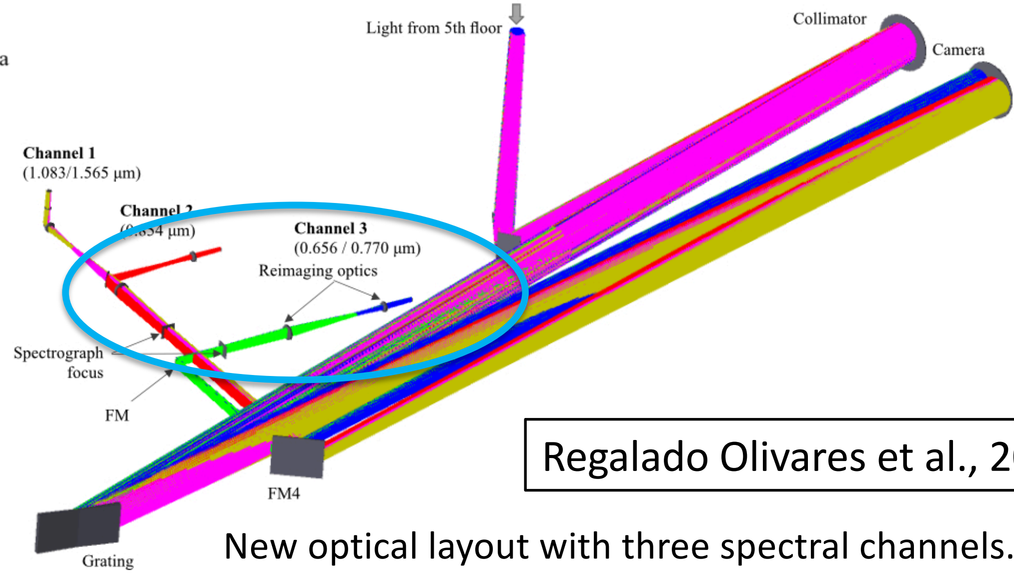

Regalado Olivares et al., 2022

New optical layout with three spectral channels.

- Two new spectral channels are included
- As a baseline, the instrument will record simultaneously <u>three spectral windows</u> centered in: λ = 0.770, 0.854 and 1.083 µm (0.770 µm channel presently in commissioning phase)

Upgrades@GREGOR: Additional simultaneous spectroscopic channels (2024)

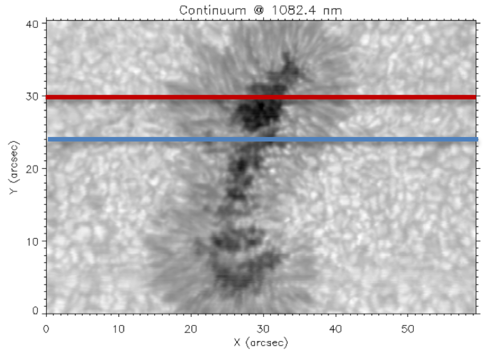

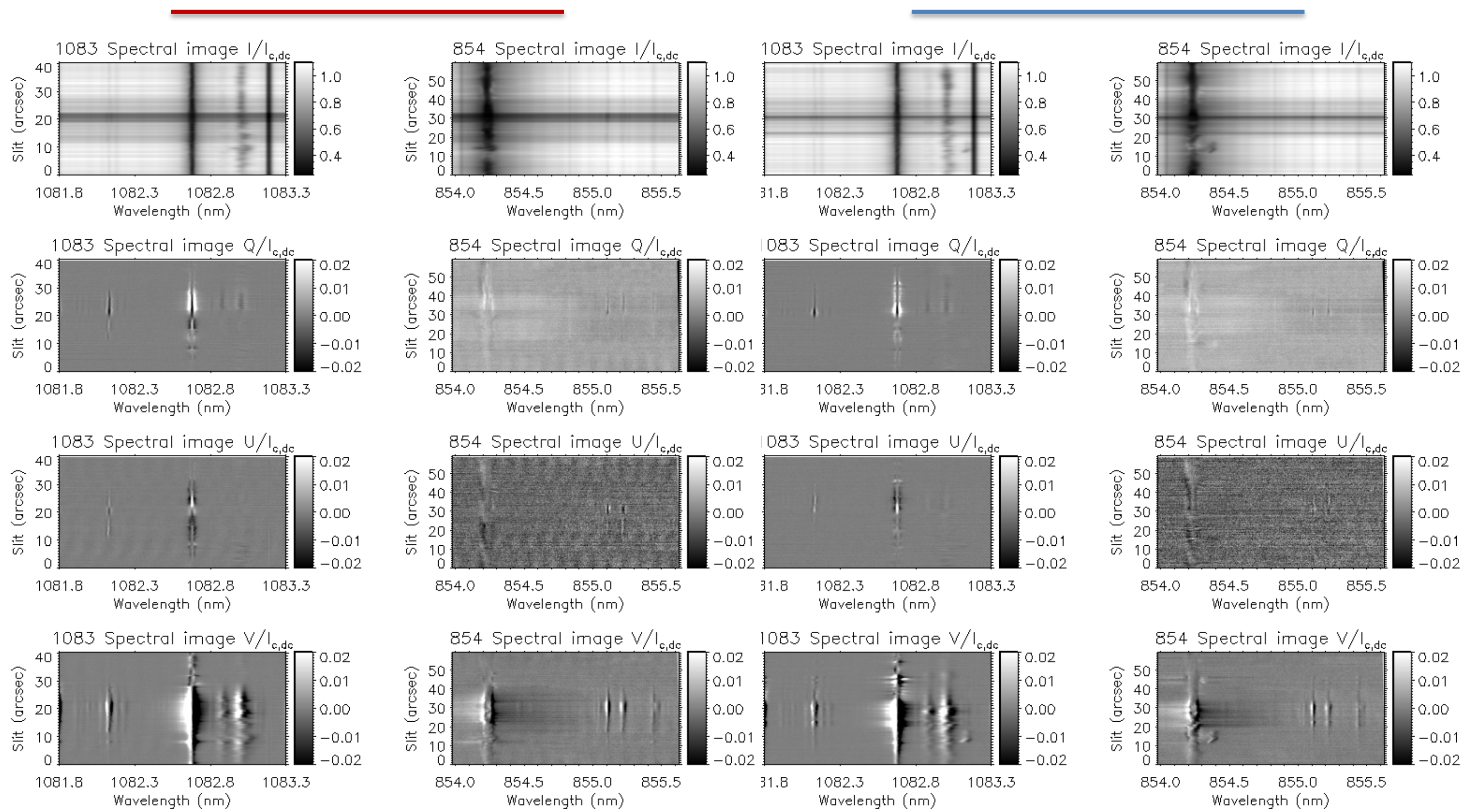

courtesy of J.C. Trelles Arjona

Upgrades@GREGOR: Additional simultaneous spectroscopic channels (2024)

Si I 1082.7 nm

He I 1083.0 nm

Ca II 854.2 nm

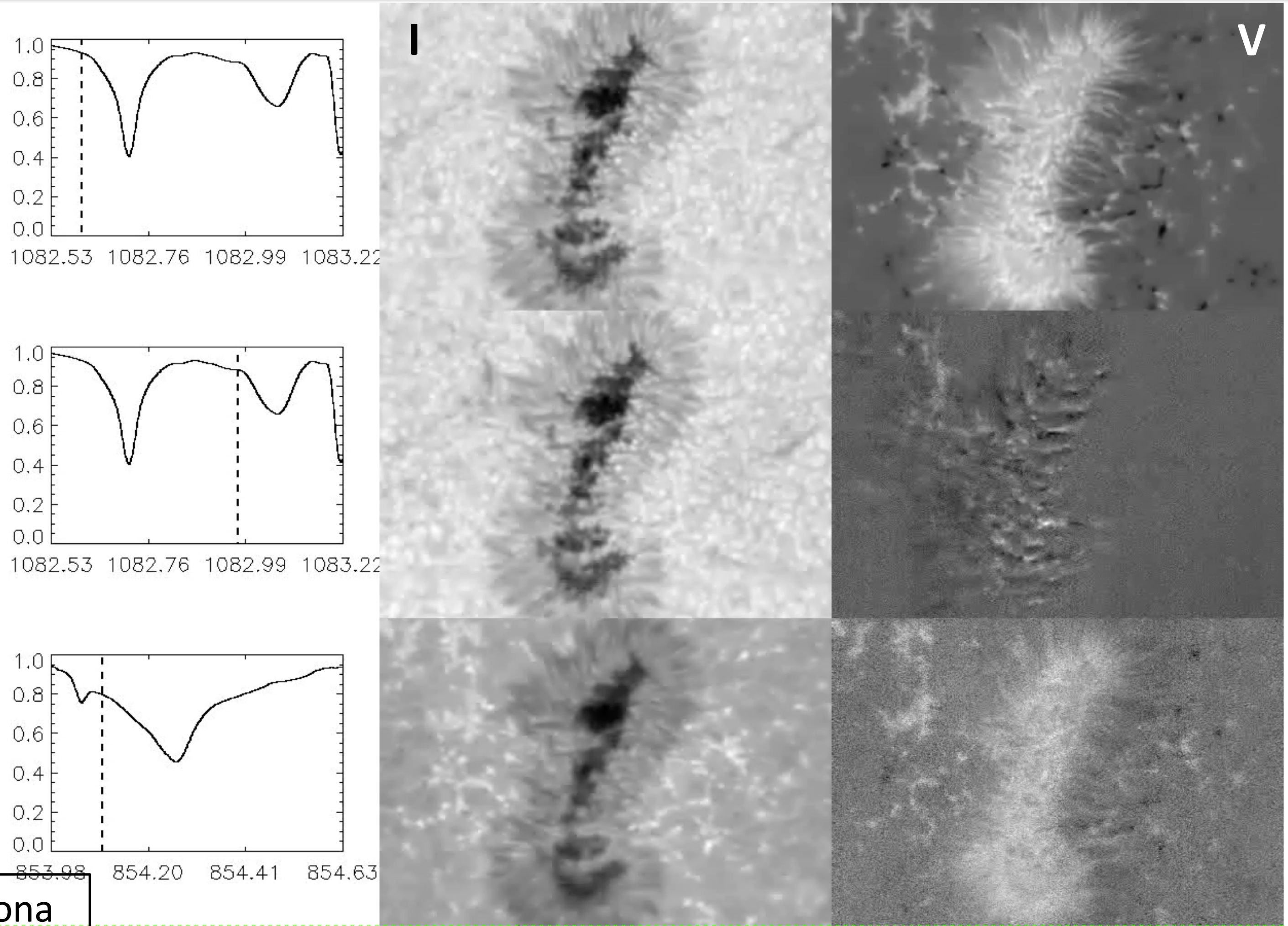

courtesy of J.C. Trelles Arjona

Upgrades@GREGOR: New AO for off-limb structures (2024)

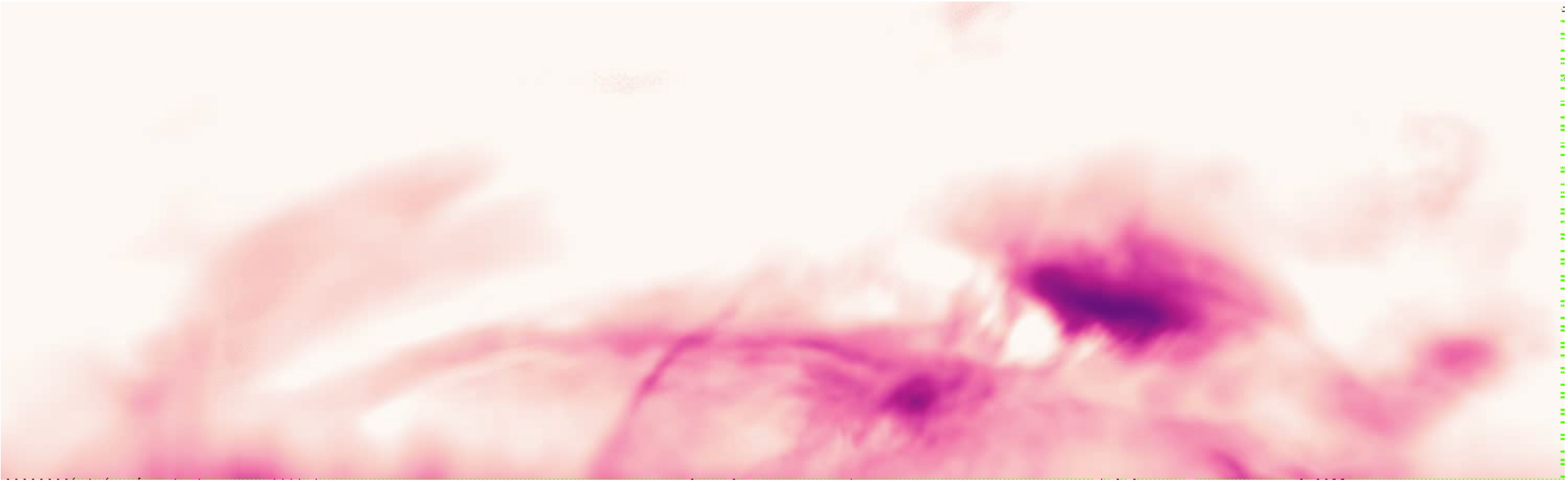

HIFI@GREGOR – Halpha (3 A wide)
courtesy of S.J. González Manrique and Ch. Kuckein

Upgrades@GREGOR: New AO for off-limb structures (2024)

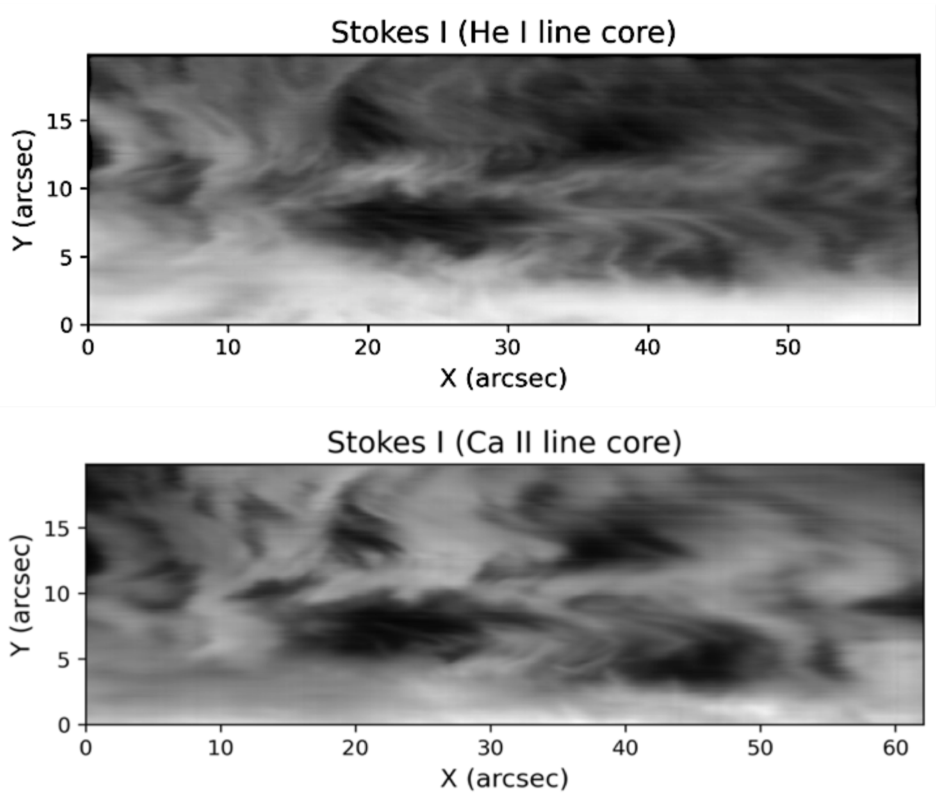

Reconstructed maps from scanning-slit

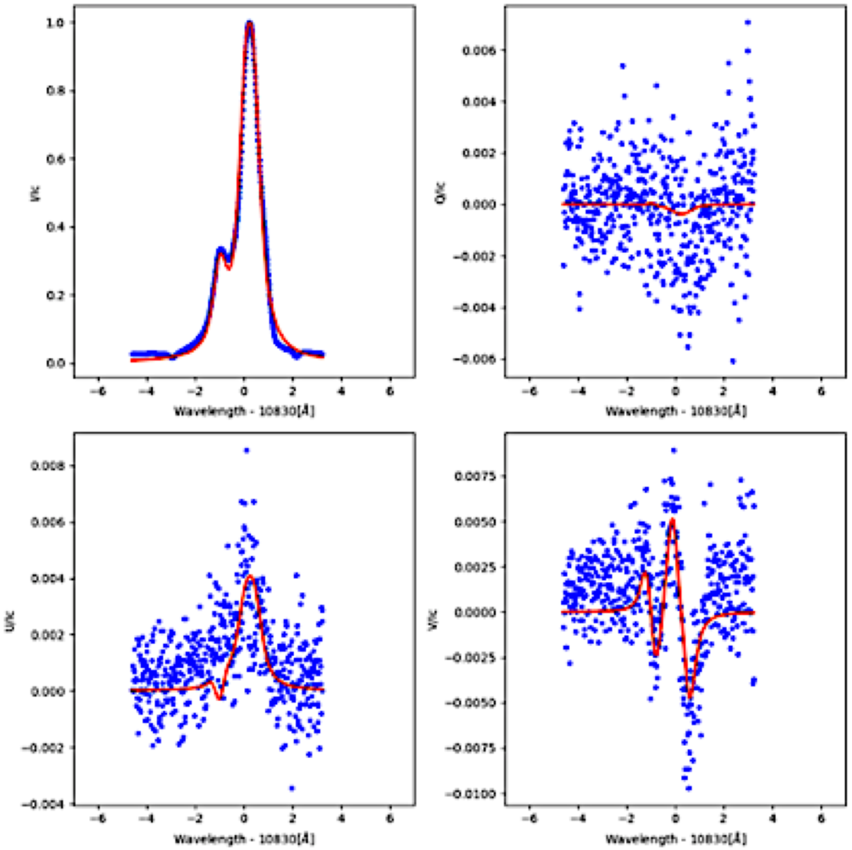

courtesy of S.J. González Manrique and Ch. Kuckein

Some statistics

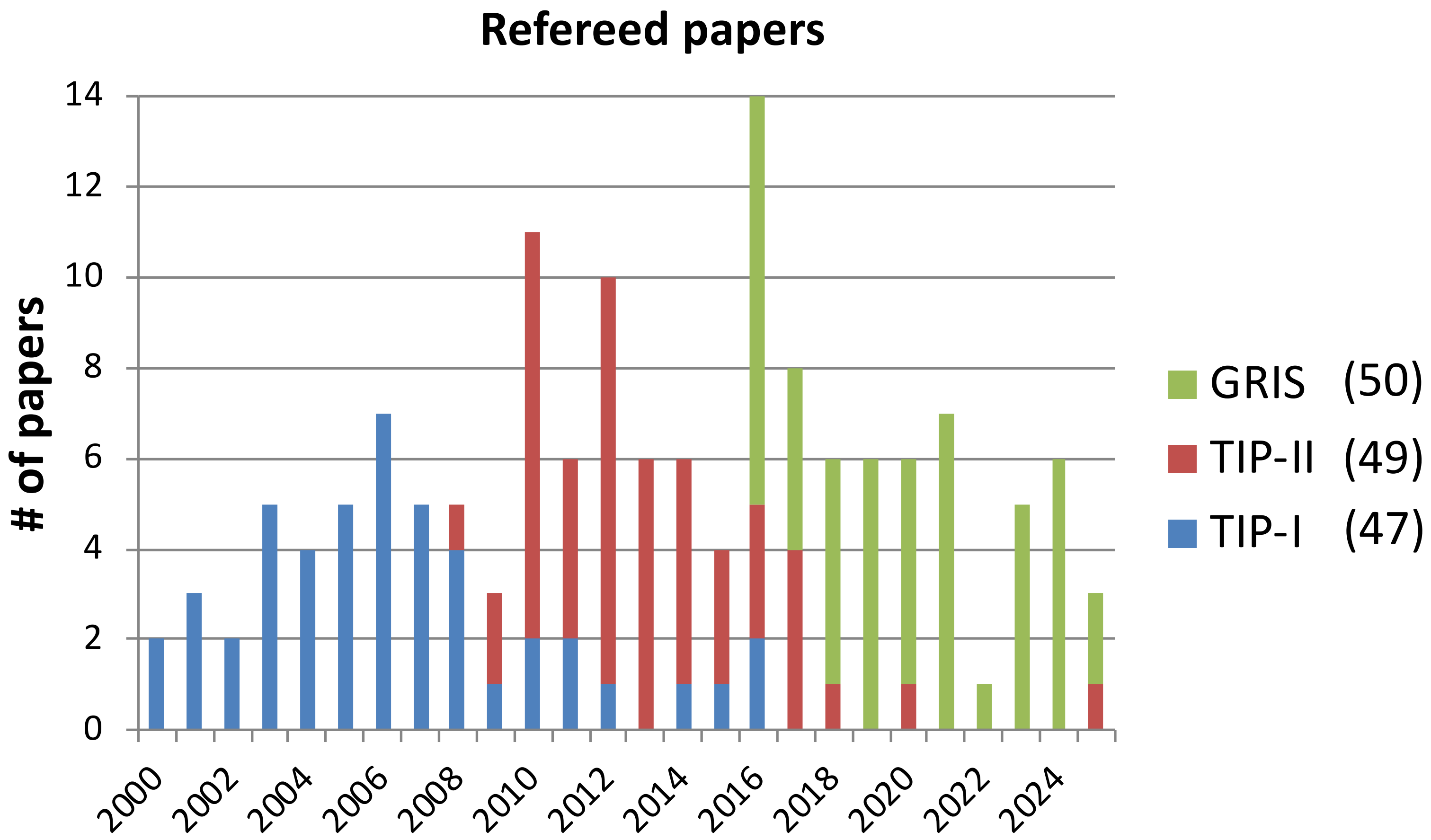

TIP-I : 1999 - 2004

TIP-II: 2005 - 2013

GRIS : 2014 - now

Some (more) statistics: 1st author institution

TIP-I

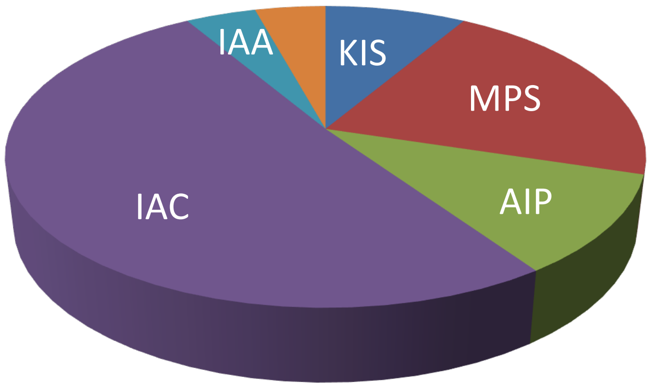

TIP-II

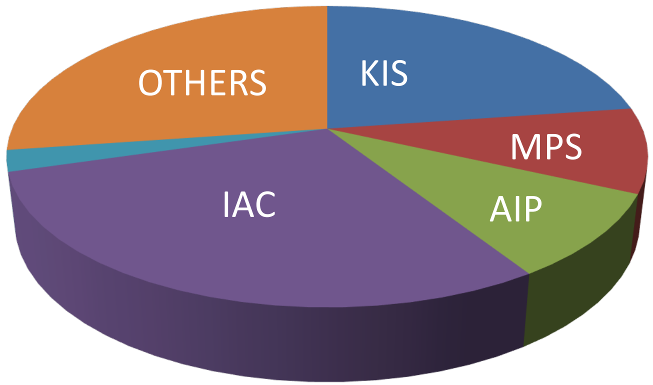

GRIS

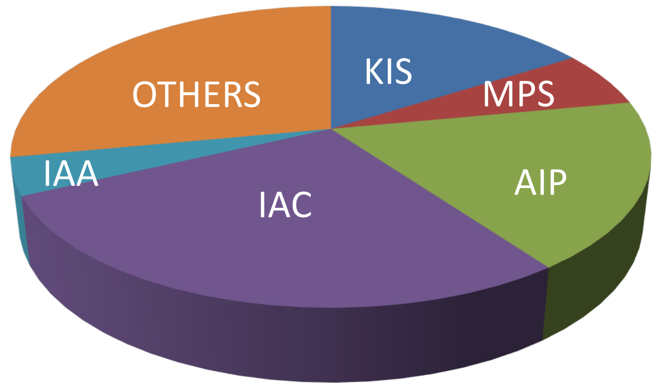

TOTAL

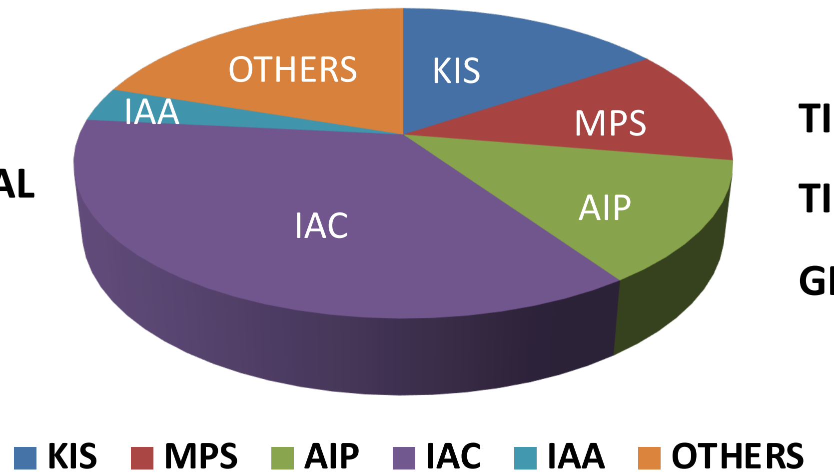

TIP-I : 1999 - 2004

TIP-II: 2005 - 2013

GRIS : 2014 - now

Collaborations DE - ES

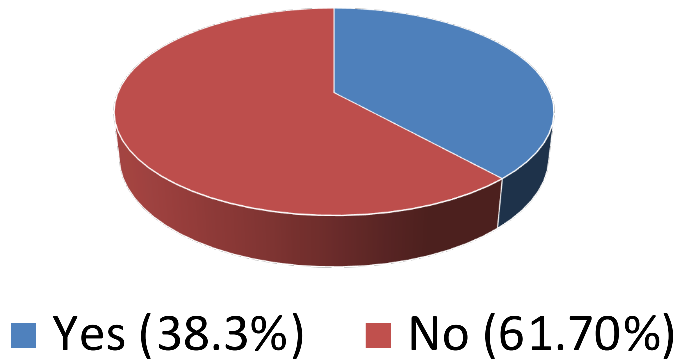

KIS Science Data Centre - Archive

https://archive.sdc.leibniz-kis.de

Instruments

- (•) GRIS@GREGOR 1605
- ( ) LARS@VTT 610
- ( ) ChroTel 201548

General

Observation Date

yyyy-mm-dd — Min: 2014-04-27

yyyy-mm-dd — Max: 2023-10-21

Observation Time

--:--:--

--:--:--

Embargo

Only Public Data

GRIS

Position on Solar Disk [Θ]

0 to 90

0 to 90

Off disc

Position on Solar Disk [μ]

0 to 1

0 to 1

Off disc

Targets

Select...

High Level Products

Inversion

Observation Type

Single Map

Time Sequence

Observation Mode

Spectroscopic

Polarimetric

Imaging System

Slit

IFU

Wavelength Region

1083nm

1565nm

Exotic wavelengths

Some (more) statistics: Topics

TOPIC	# refereed papers	TOPIC	# refereed papers
Quiet Sun	25	Waves and Oscillations	19
Sunspot Structure	23	Emerging regions (arch filament system)	12
Penumbral Structure	20	Filaments/Prominences	16
Light-Bridges	4	Spicules	5
Active Regions	5	Flares	3
Others	22		

Science objectives

- Quiet Sun magnetism
- Active regions, sunspot structure, penumbra
- Photospheric-chromospheric magnetic field topology
- Emerging regions – Arch Filament Systems
- Wave propagation
- Chromospheric activity: Flares, Filaments, prominences, spicules
- …

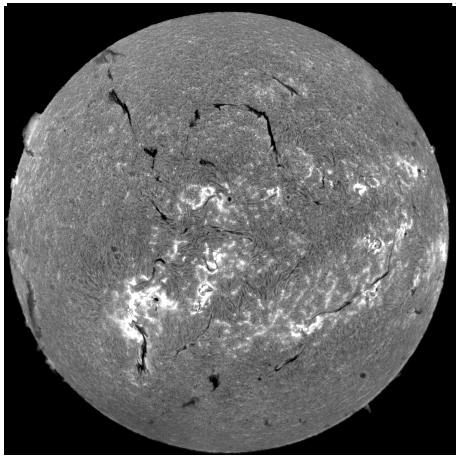

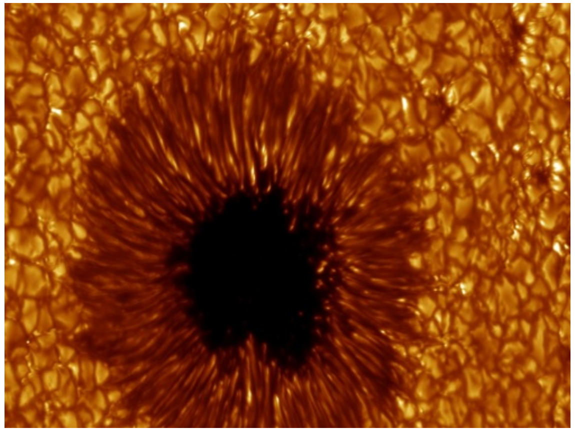

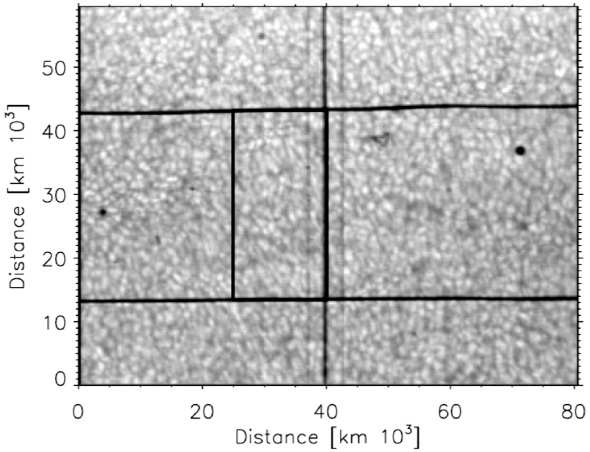

Some relevant results: magnetic fields in the very quiet sun

Magnetic fields in the very quiet sun:

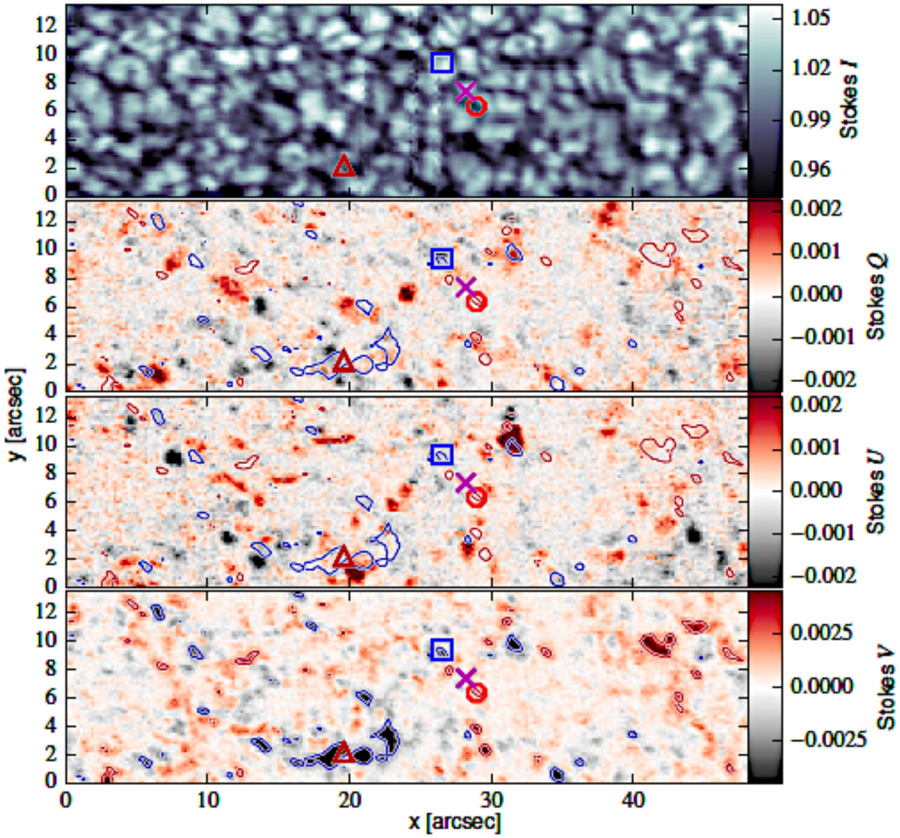

Table 1. Percentage of linear (LP) and circular (CP) polarization profiles above a certain σ-threshold for GRIS and SOT/SP data sampled at 0″.20.

σ-level	GRIS [%] LP	CP	LP and CP	LP or CP	SOT/SP [%] LP	CP	LP and CP	LP or CP
3σ	39.7	73.0	33.1	79.7	9.8	49.3	7.7	51.4
4σ	18.4	57.0	13.9	61.5	4.2	37.1	3.1	38.2
5σ	9.2	44.2	6.2	47.2	2.1	28.5	1.5	29.1

- About 80% of the GRIS spectra of a very quiet solar region show polarimetric signals above a 3 level.
- Area and amplitude asymmetries agree well with small-scale surface dynamo-magneto hydrodynamic simulations.
- The magnetic line ratio analysis reveals ubiquitous magnetic regions in the ten to hundred Gauss range with some concentrations of kilo-Gauss fields.

Lagg et al (2016)

Solar-cycle and Latitude Variations in the Internetwork Magnetism

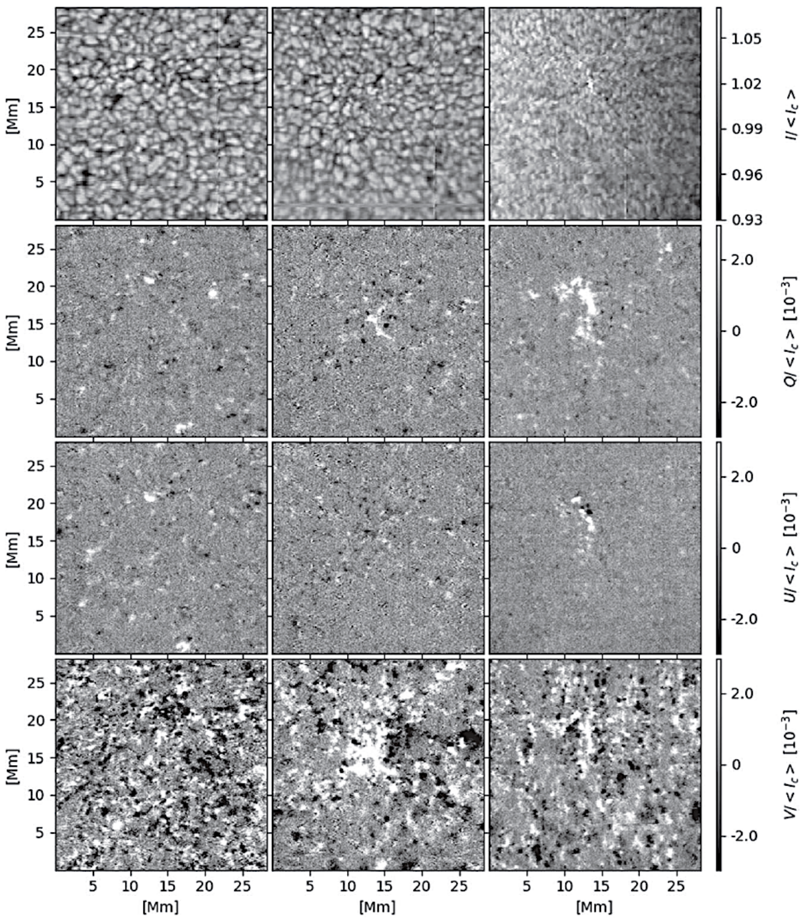

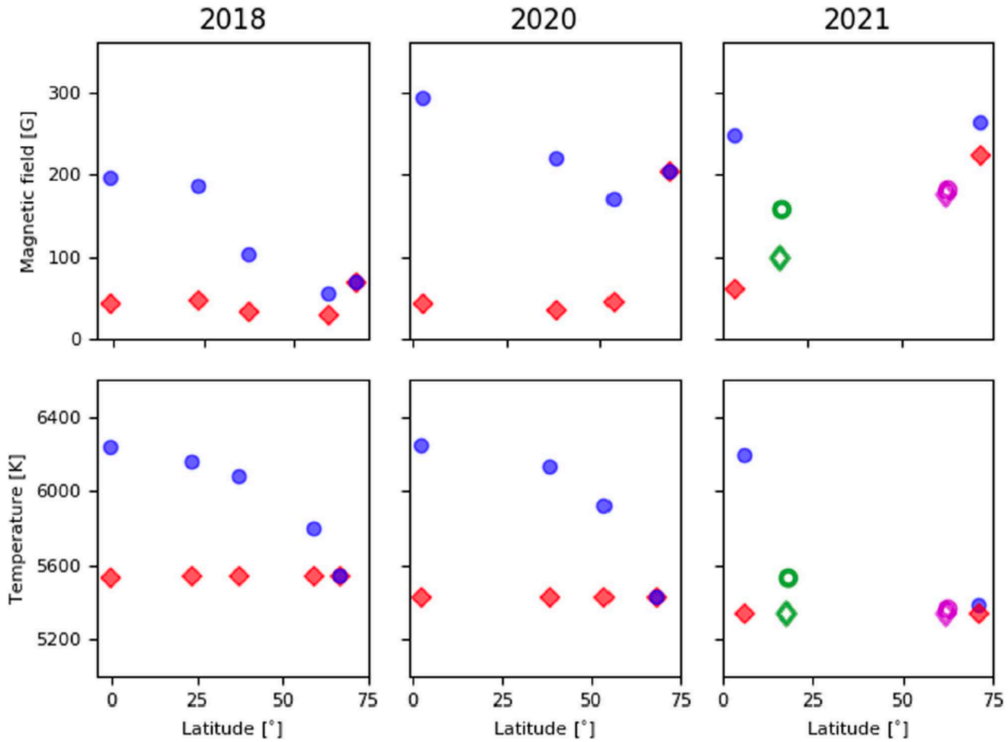

Blue circles: no correction for differential layers (N-S)
Red Diamonds: correction applied for same layer (N-S)
Green Diamonds: E-W (equator)

Trelles Arjona et al. (2023)

Mapping the Hidden Magnetic Field of the Quiet Sun

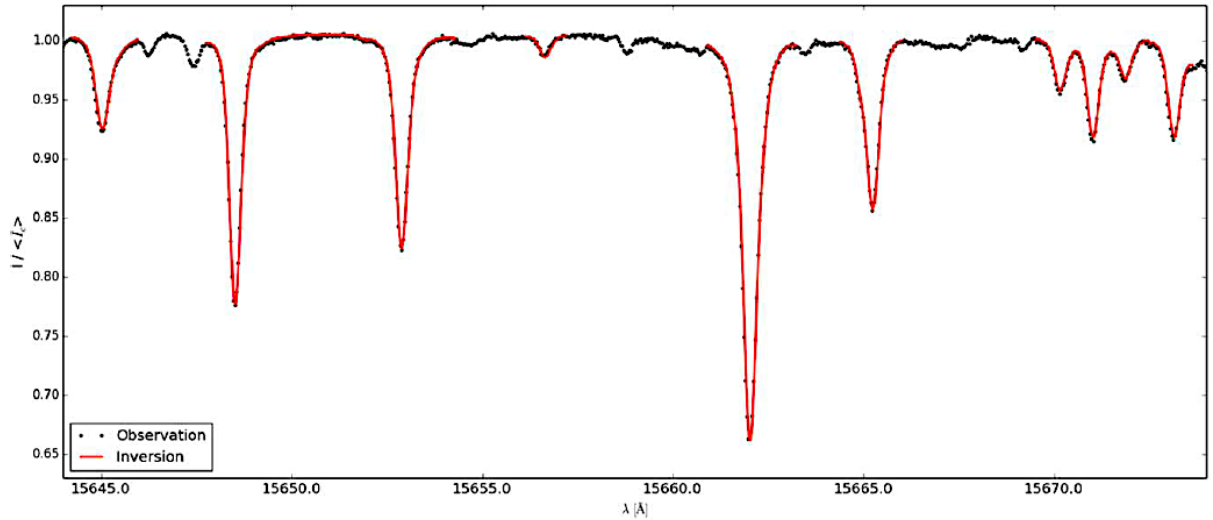

- Multi-line intensity profiles
- No polarization information used!!!

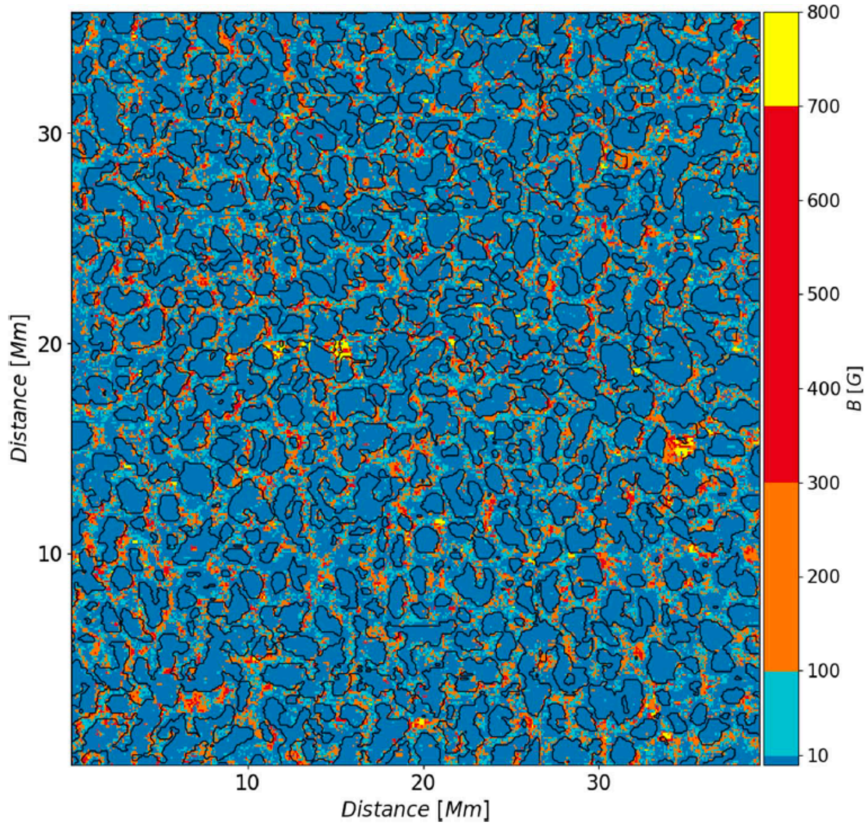

Trelles Arjona et al. (2021)

Sunspot penumbra: no evidence of field-free

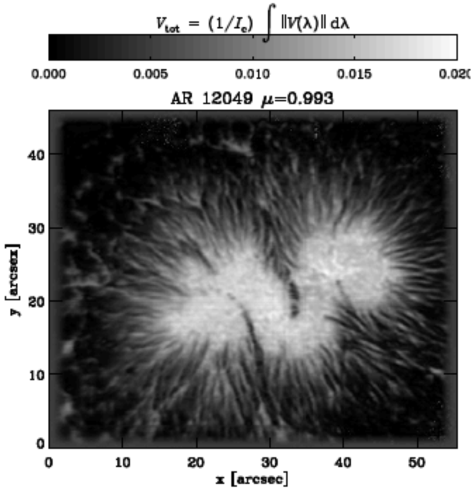

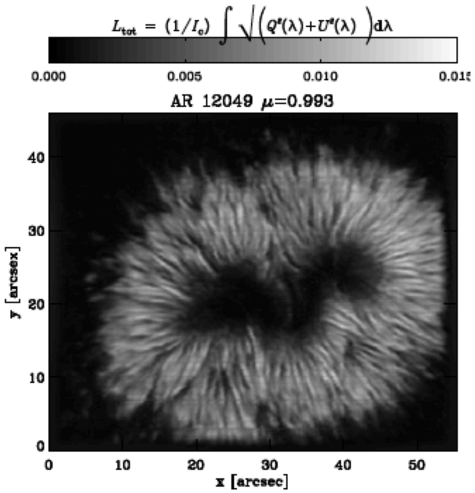

Sunspot penumbra: no evidence of field-free gaps

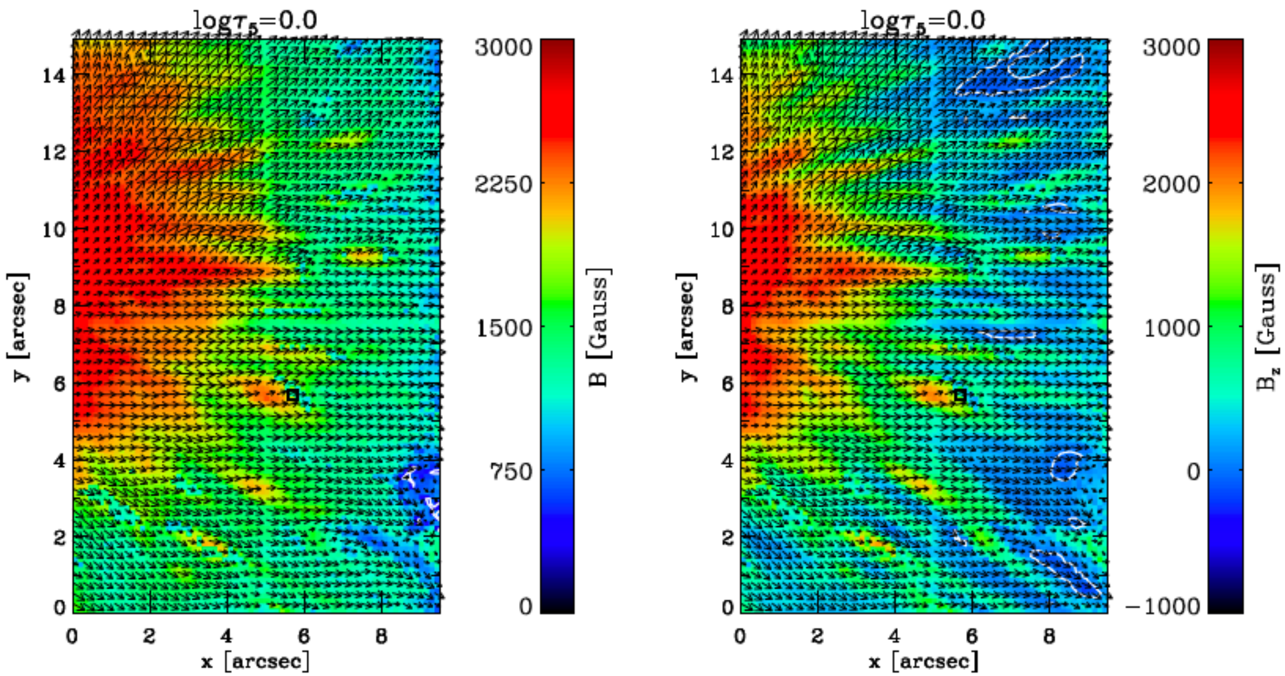

Borrero et al (2016)

Three-dimensional structure of a sunspot light bridge

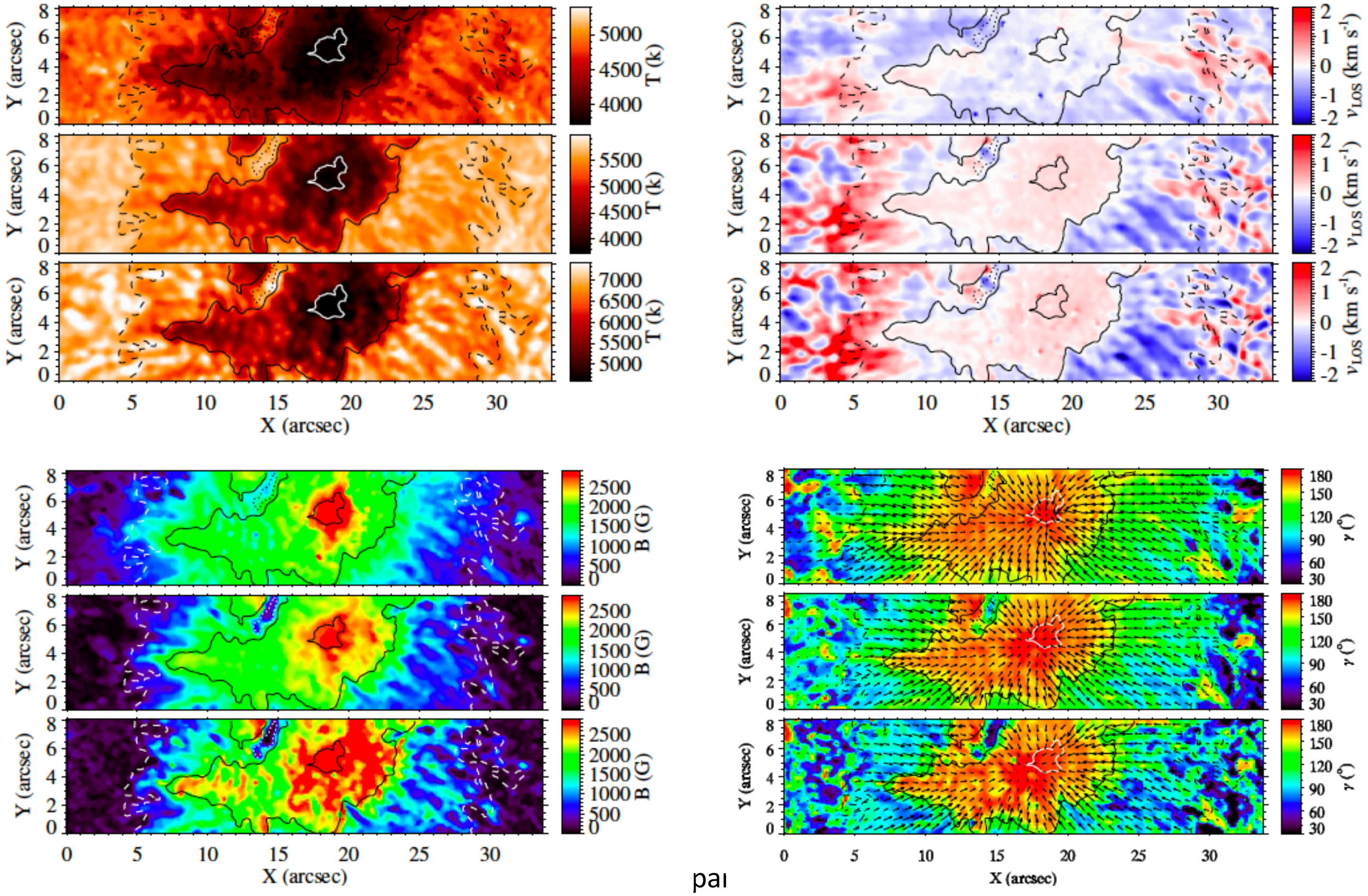

log(tau) = -2.2

log(tau) = -0.5

log(tau) =   0.3

log(tau) = -2.2

log(tau) = -0.5

log(tau) =   0.3

Felipe et al. (2016)

pai

Three-dimensional structure of a sunspot light bridge

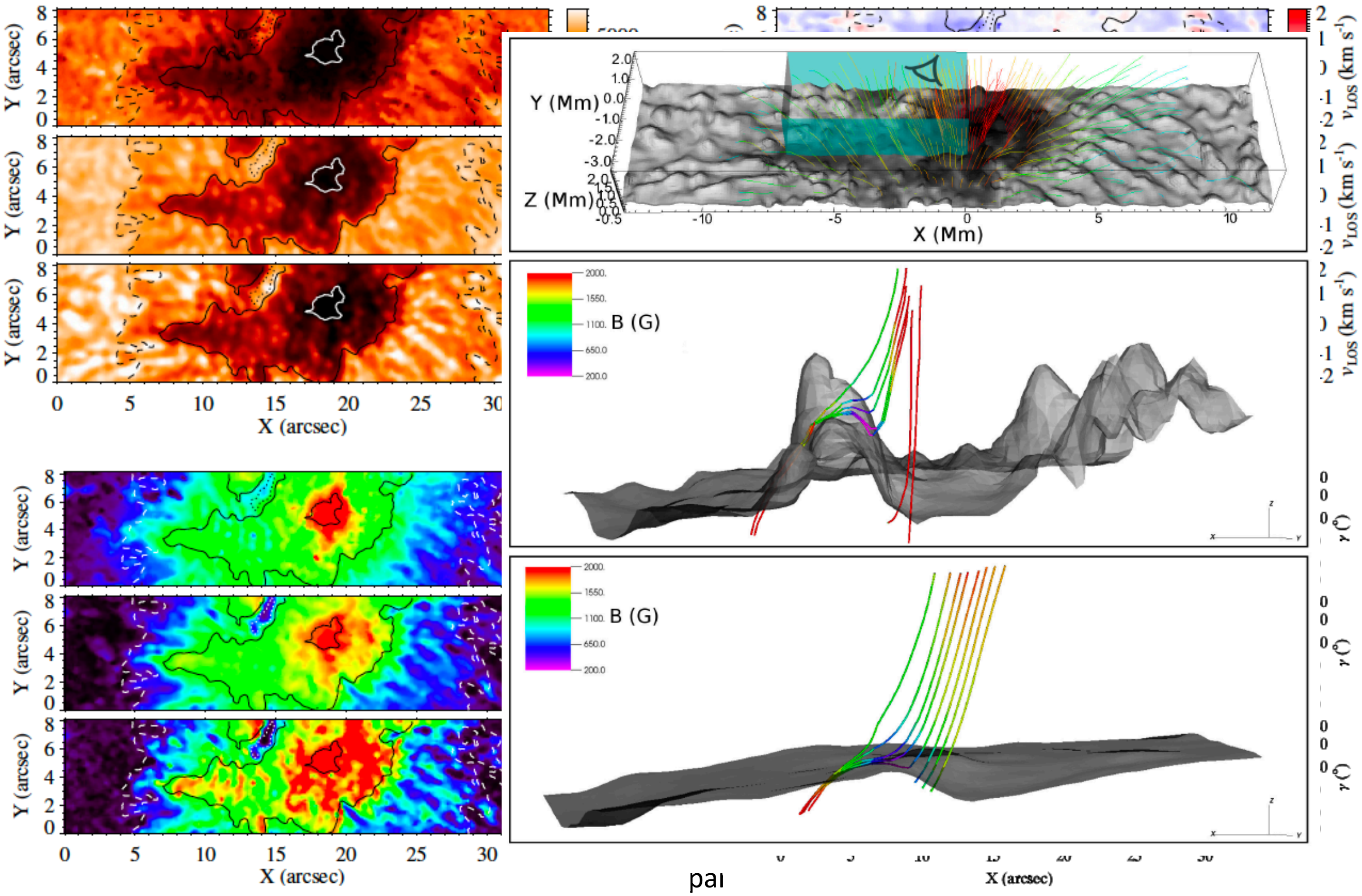

log(tau) = -2.2

log(tau) = -0.5

log(tau) = 0.3

log(tau) = -2.2

log(tau) = -0.5

log(tau) = 0.3

Felipe et al. (2016)

Characterization of the umbra–penumbra boundary by the vertical component of the magnetic field

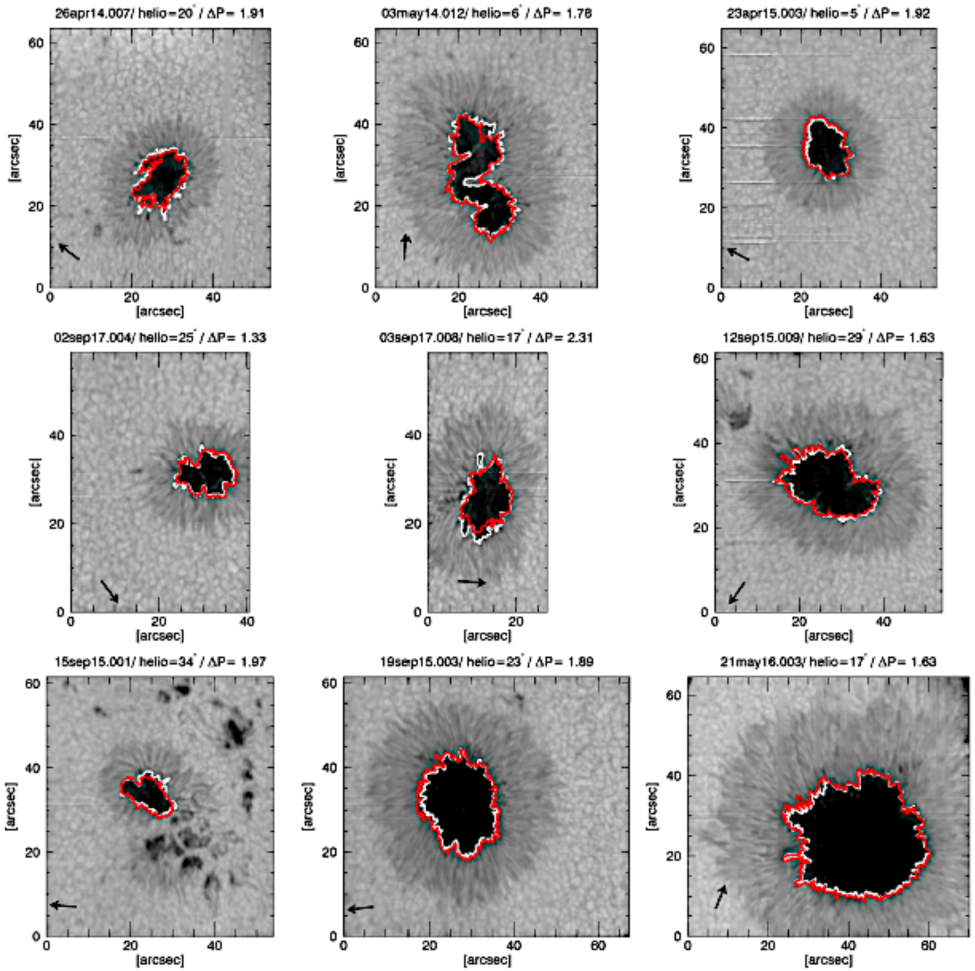

Umbra-penumbra interface

$$B_z = 1787 \ \pm 100\ G$$

Lindner et al (2020)

Height variation of the cutoff frequency in a sunspot umbra

a) Ca I 10839 A (GRIS)

b) Fe I 5435 A (GFPI)

c) He I 10830 (GRIS)

d) Si 10827 (GRIS)

. Our measurements show that between the deep photosphere and high photosphere the cut-off frequency increases from 5 mHz to 6 mHz. At higher chromospheric values the cutoff is reduced to ~3.1 mHz. These results have been compared with the values obtained from the application of several analytical cutoff forms to the atmosphere inferred from the inversion of the photospheric lines and to a standard model of umbral stratification. This comparison reveals some significant differences at the photosphere.

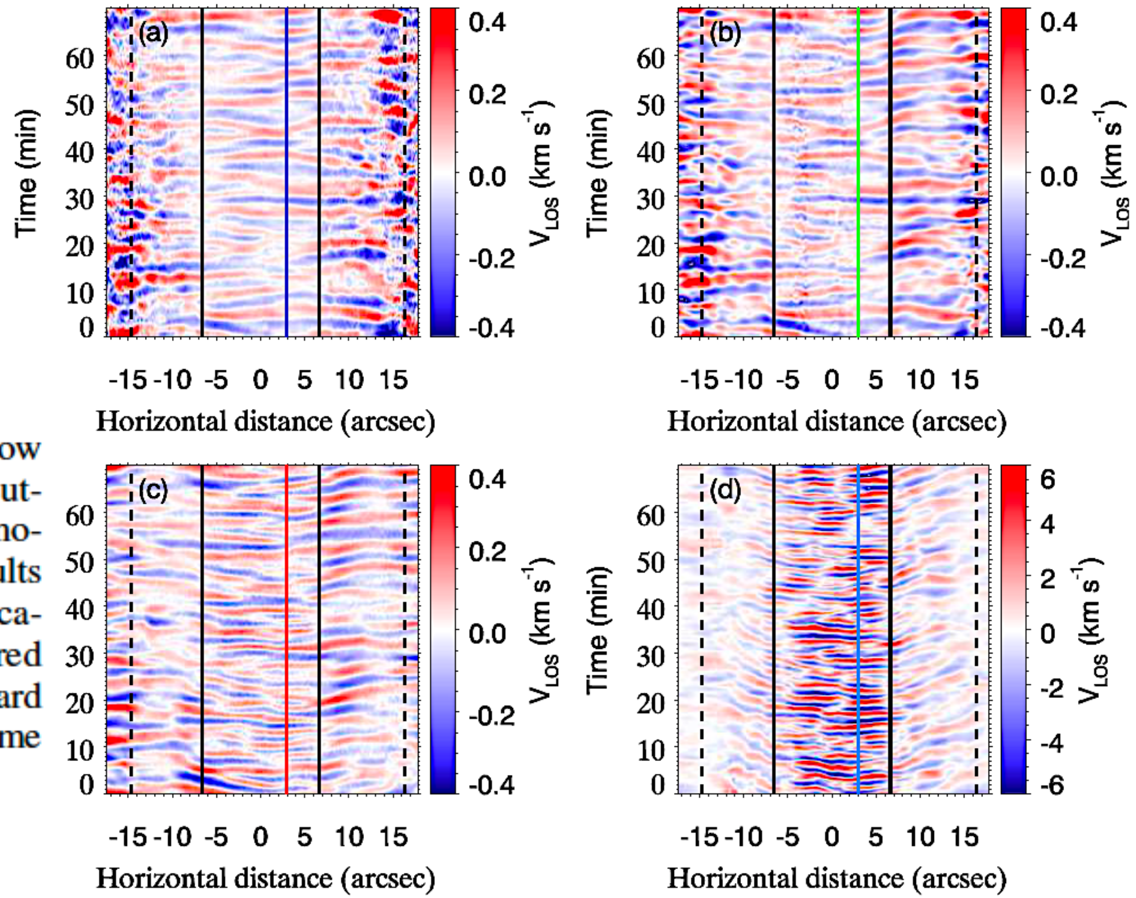

Felipe et al (2018)

Tracking Downflows from the Chromosphere to the Photosphere in a Solar Arch Filament System

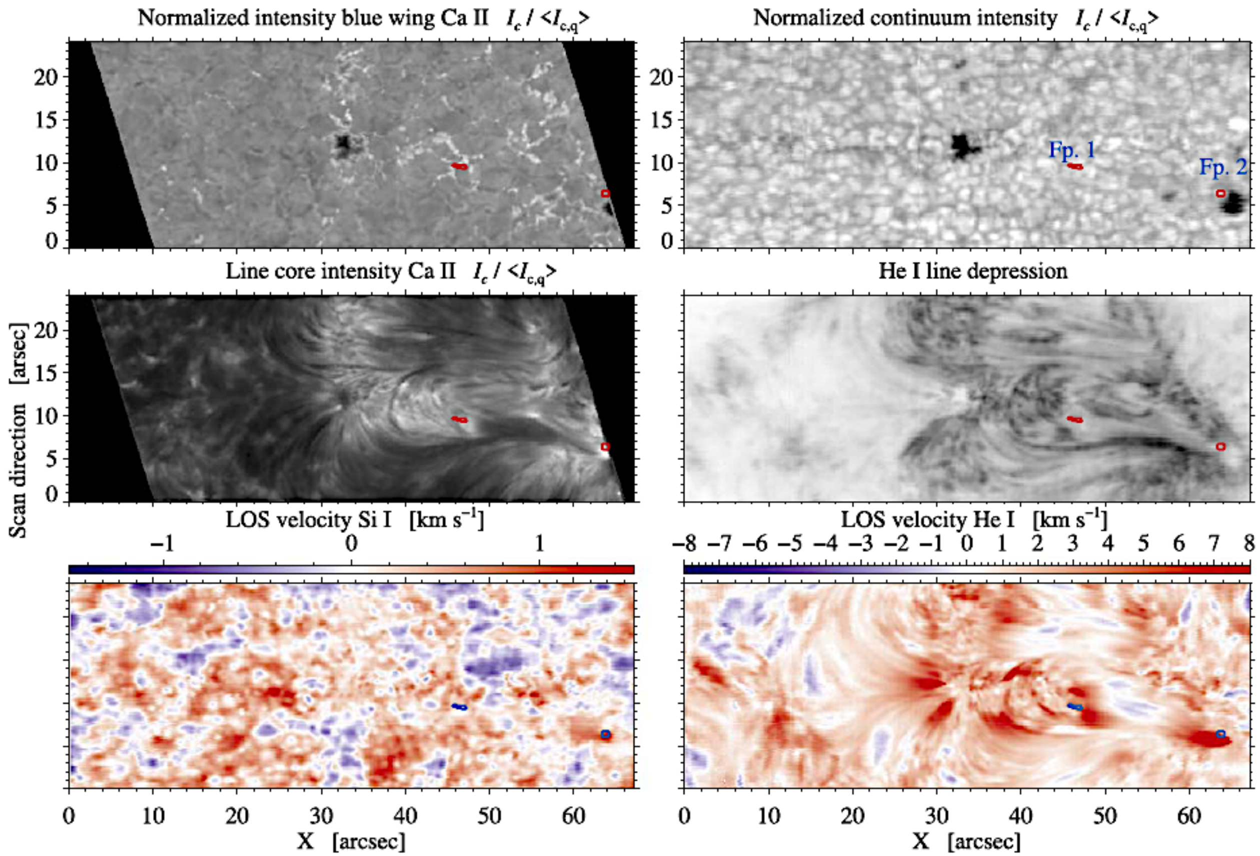

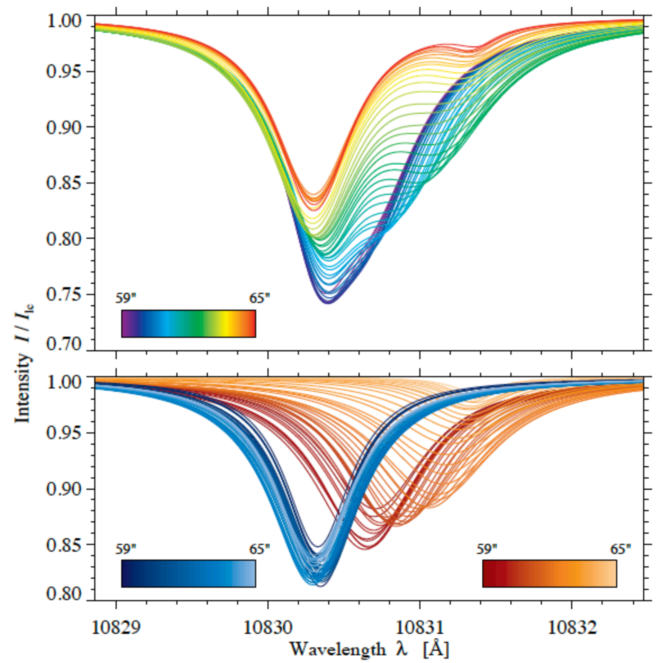

González Manrique et al (2016, 2020)

Tracking Downflows from the Chromosphere to the Photosphere in a Solar Arch Filament System

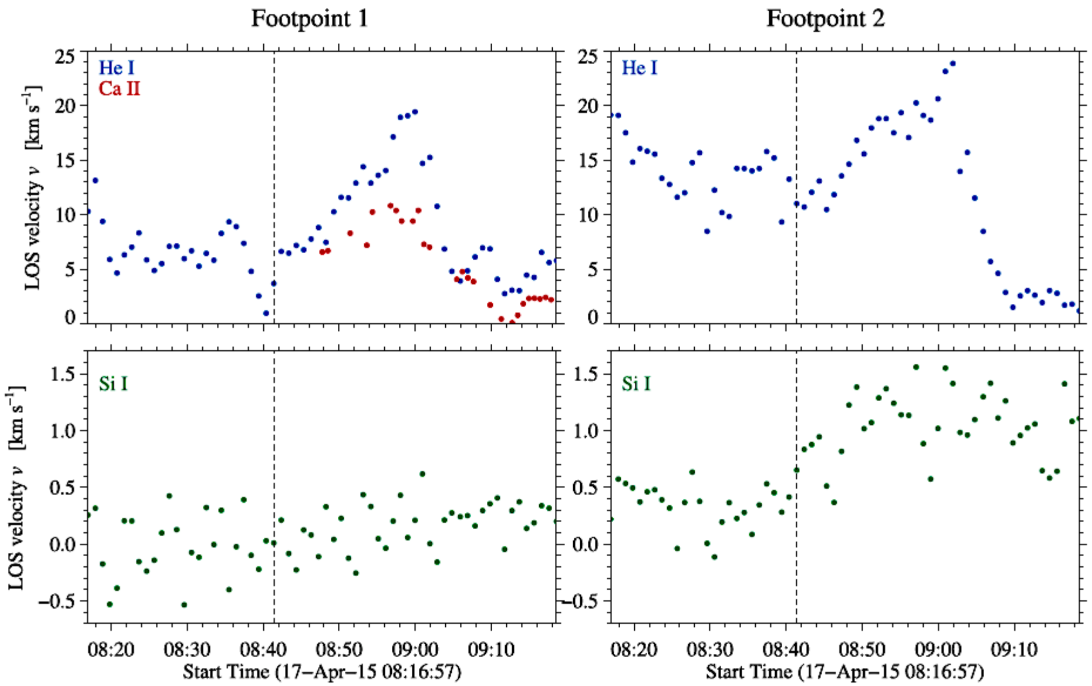

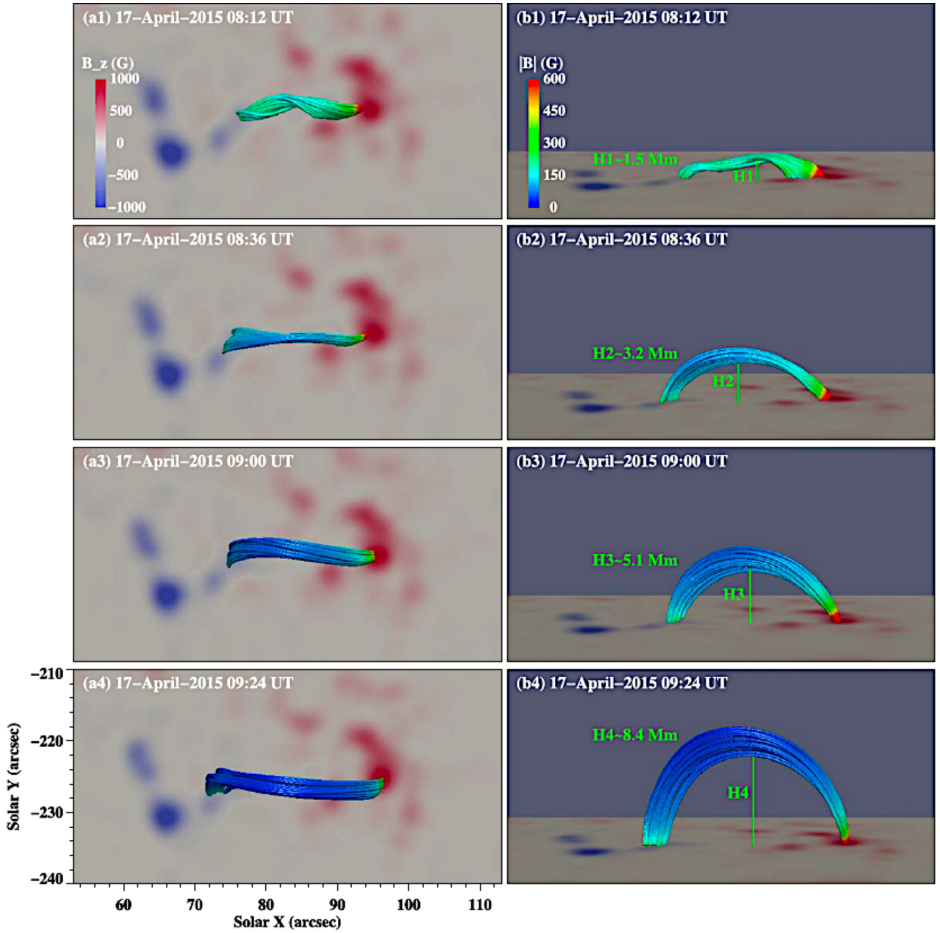

González Manrique et al (2020)

Determining the dynamics and magnetic fields in He I 10830 Å during a solar filament eruption★

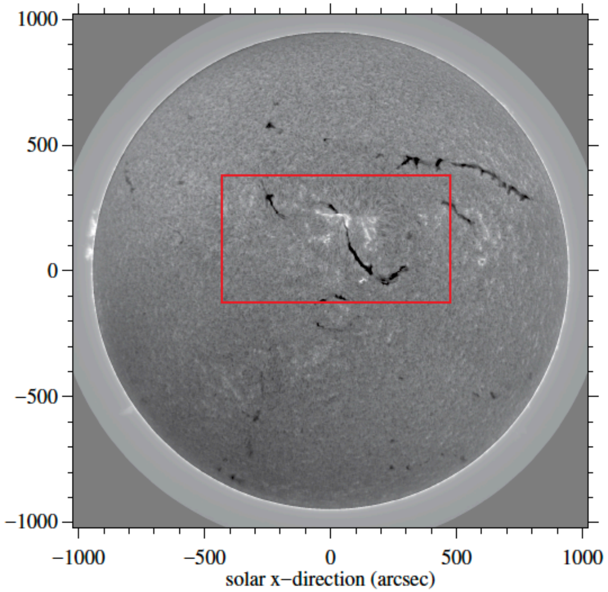

ChroTEL Hα image

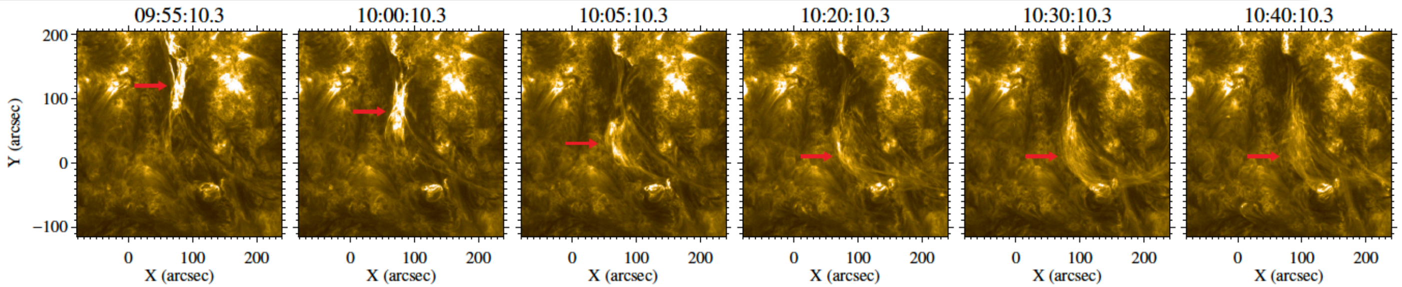

AIA 171 filtergrams

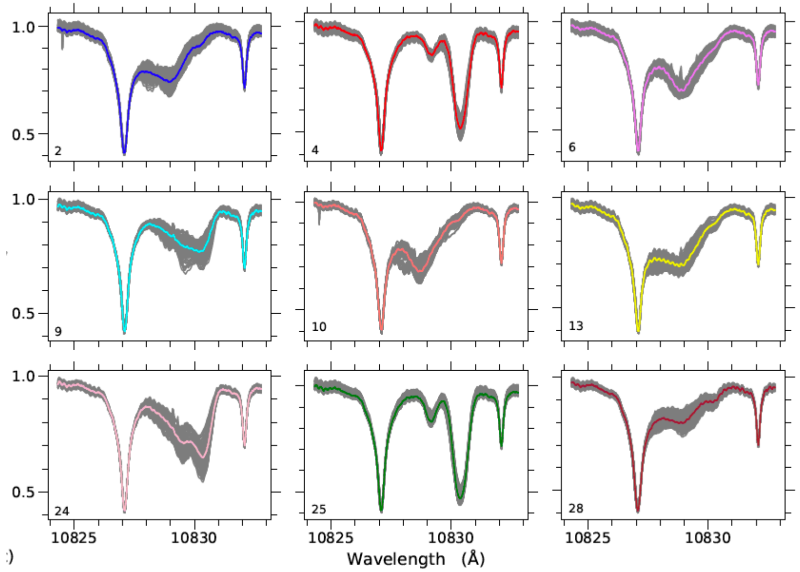

GRIS 1083 spectra

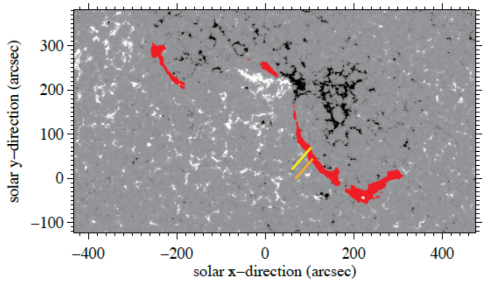

HMI magnetogram

Kuckein et al (2020)

SUMMARY

GRIS is a very versatile instrument:

- It can be used in long-slit or IFU configuration
- It has multiwavelength capabilities
- It has polarimetric capabilities
- It can provide height-dependent information
- It can be easily combined with other instruments
- Data are freely accesible at KIS SDC webpage